Western Graduate&PostdoctoralStudies

Western University
Scholarship@Western

Electronic Thesis and Dissertation Repository

4-18-2012 12:00 AM

Investigation of histone lysine methylation in stem cell differentiation using inhibitor peptide

Wendy Zhu, *The University of Western Ontario*

Supervisor: Dr. Shawn Li, *The University of Western Ontario*

A thesis submitted in partial fulfillment of the requirements for the Master of Science degree in Biochemistry

© Wendy Zhu 2012

Follow this and additional works at: https://ir.lib.uwo.ca/etd

Part of the Biological Phenomena, Cell Phenomena, and Immunity Commons

Recommended Citation

Zhu, Wendy, "Investigation of histone lysine methylation in stem cell differentiation using inhibitor peptide" (2012). *Electronic Thesis and Dissertation Repository*. 496.
https://ir.lib.uwo.ca/etd/496

This Dissertation/Thesis is brought to you for free and open access by Scholarship@Western. It has been accepted for inclusion in Electronic Thesis and Dissertation Repository by an authorized administrator of Scholarship@Western. For more information, please contact wlswadmin@uwo.ca.

INVESTIGATION OF HISTONE LYSINE METHYLATION IN STEM CELL DIFFERENTIATION USING INHIBITOR PEPTIDE

(Spine title: Inhibitor peptide in stem cell epigenetics)

(Thesis format: Integrated Article)

by

Wendy Zhu

Graduate Program in Biochemistry

A thesis submitted in partial fulfillment
of the requirements for the degree of
Master of Science

The School of Graduate and Postdoctoral Studies
The University of Western Ontario
London, Ontario, Canada

© Wendy Zhu 2012

THE UNIVERSITY OF WESTERN ONTARIO
School of Graduate and Postdoctoral Studies

CERTIFICATE OF EXAMINATION

Supervisor

Dr. Shawn Li

Supervisory Committee

Dr. Madhulika Gupta

Dr. Mellissa Mann

Examiners

Dr. David Litchfield

Dr. Megan Davey

Dr. Lynne Postovit

The thesis by

Wendy Zhu

entitled:

INVESTIGATION OF HISTONE LYSINE METHYLATION IN STEM CELL DIFFERENTIATION USING PEPTIDE INHIBITOR

is accepted in partial fulfillment of the
requirements for the degree of
Masters of Science

Date

Chair of the Thesis Examination Board

Abstract

In an effort to expand the histone code, we examine a novel site of methylation on lysine 43 of histone H2B. In mouse embryonic stem cells (ESCs), KDM5b acts as the lysine demethylase for H2BK43me2, diminishing this histone mark as cells differentiate. We utilize a synthetic peptide mimetic corresponding to amino acids 37-49 of histone H2B in order to sterically inactivate KDM5b enzyme. The addition of inhibitor peptide into culture enhanced stem cell differentiation, upregulating cell cycle and neural-specific markers while downregulating the expression of pluripotency genes. Global gene analysis patterns of peptide-treated ESCs were representative of differentiated cell populations. Applying a novel inhibition method, we reveal an accelerated rate of stem cell differentiation through the upregulation of KDM5b targets. Our investigation serves to elucidate the role of histone H2BK43 methylation in an epigenetically regulated model of development.

Keywords

Mouse embryonic stem cells, epigenetics, lysine methylation, cell differentiation, development, peptide inhibition, H2B histone, KDM5b, chromatin immunoprecipitation

Co-Authorship Statement

All experiments were performed by Wendy Zhu, with the exception of the following: Figure 2.1A MALDI-MS was accomplished with the assistance of Dr. Marek Galka. Figure 2.8 microarray and gene ontology analysis was obtained with the assistance of Rich Carpenado and Dr. Willian Stanford's lab at the University of Toronto. Figure 2.9A Western blot was performed in collaboration with Leanne Stalker at McMaster University.

Acknowledgments

I would like to give acknowledgement to the following people who have contributed my Master's project:

First and foremost, I thank my supervisor Dr. Shawn Li for providing me with an enriched environment for education.

I would like to extend my greatest appreciation to Dr. Christopher Wynder for his wonderful guidance. I am both appreciative and very fortunate to have had you as my valuable mentor.

I also thank Dr. Huadong Liu and Dr. Marek Galka for assisting my learning experience, and to the rest of the Li Lab for making the past few years so enjoyable.

Lastly, I thank my family for the unconditional support, and my friends for the perpetual inspiration.

Table of Contents

CERTIFICATE OF EXAMINATION ii

Abstract and Keywords iii

Co-Authorship Statement/Acknowledgements iv

Table of Contents v

List of Figures viii

List of Abbreviations and Nomenclature ix

Chapter 1: Literature Review 1

1.1 Embryonic stem cell model 1

1.2 Maintenance of pluripotency 2

1.3 Cell cycle control in cancer and development 3

1.4 Epigenetic gene regulation 7

1.5 The Histone Code 8

1.6 Lysine methylation and chromatin remodeling 9

1.7 Histone lysine demethylases 10

1.8 PLU1/JARID1B/KDM5b 15

1.9 Histone H2B 16

1.10 H2BK43 demethylation via KDM5b 17

1.11 Applications of peptide mimetic 18

1.12 Hypothesis and outline 19

References 21

Chapter 2: Histone lysine methylation in stem cell differentiation 32

2.1 Introduction 32

2.2 Methods 33

2.2.1 Cell culture 33

2.2.2 Differentiation assay 34

2.2.3 Peptide synthesis 35

2.2.4 HPLC purification 35

2.2.5 MALDI-MS and Gene Ontology analysis 36

2.2.6 Immunocytochemistry 36

2.2.7 Immunoprecipitation and Western blot 37

2.2.8 Quantitative RT-PCR 37

2.2.9 Chromatin Immunoprecipitation (ChIP) 38

2.2.10 Statistical analysis 38

2.3 Results 40

2.3.1 Synthetic peptides exhibited nuclear localization in ESCs 40

2.3.2 ESCs formed neurospheres upon LIF withdrawal and aggregation 40

2.3.3 H2BK43 peptide promoted a neural phenotype in ESCs 45

2.3.4 Neural phenotype was specific to H2BK43me0 peptide 45

2.3.5 H2BK43me0 treatment downregulated pluripotency factor Nanog and induced expression of neural markers 50

2.3.6 Peptide-treated ESCs upregulated expression of cell cycle gene Egr1 50

2.3.7 Peptide-induced differentiation upregulated BRCA1, Synapsin, and Sox17 but not TRAIL 53

2.3.8 Microarray analysis revealed characteristics in peptide-treated ESCs similar to differentiated cells 58

2.3.9 H2BK43me0 peptide inhibited KDM5b demethylase activity 58

2.3.10 Peptide treatment upregulated H2BK43me2 recruitment at Egr1 promoter regions 61

2.4 Discussion 66

2.4.1 Inhibitor peptide localized into ESCs and induced transcriptional changes resulting in differentiation 66

2.4.2 H2BK43me0 peptide is an inhibitor of KDM5b and upregulates known target genes 68

2.4.3 Global gene expression of peptide-treated cells recapitulate changes in KDM5b heterozygous ESCs 70

2.4.4 Recruitment of KDM5b substrates increased in cells treated with inhibitor peptide 71

2.4.5 Peptide-induced cell differentiation is specific to H2BK43me0 72

Chapter 3: General Overview 81

3.1 Conclusion and Summary 81

3.2 Future Studies 84

References 87

Curriculum Vitae 90

List of Figures

1.1 Cell cycle control genes regulate proliferation versus differentiation.....5

1.2 Structural domains of PLU1/JARID1B/KDM5b.....13

2.1 H2BK43me0 inhibitor peptides were confirmed, purified, and nuclear-localized in ESCs.....41

2.2 Mouse embryonic stem cells begin differentiating upon LIF withdrawal and form neurospheres when aggregated.....43

2.3 Incubating ESCs with H2BK43me0 peptide induced a neural differentiation phenotype.....46

2.4 Treatment of H2BK43me3, H3K4 and H3K9 peptides did not promote any changes in ESC morphology.....48

2.5 ESCs incubated with peptide inhibitor exhibited downreguation of Nanog and upregulation of neural markers.....51

2.6 H2BK43me0 peptide treatment resulted in the early upregulation of Egr1 compared to TAT treatment.....54

2.7 ESCs incubated with inhibitor peptide upregulated lineage genes but did not express apoptosis factor TRAIL.....56

2.8 Gene Ontology analysis revealed differences between TAT and H2BK43me0-treated ESCs.....59

2.9 H2BK43me0 peptide inhibits KDM5b and affects transcriptional regulation of TCF3.....62

2.10 Peptide treatment recruited H2BK43me2 at Egr1 promoter regions similar to differentiated cells.....64

List of Abbreviations and Nomenclature

bHLH	basic helix-loop-helix
BRCA1	breast cancer type 1 susceptibility protein
CDK	cyclin-dependent kinase
ChIP	chromatin immunoprecipitation
DMEM	Dulbecco's modified eagle medium
Dnmt	DNA methyltransferase
Egr1	early growth response protein 1
ESC	embryonic stem cell
GAPDH	glyceraldehyde 3-phosphate dehydrogenase
GO	gene ontology
HAT	histone acetyltransferase
HDAC	histone deacetylase
HIV	human immunodeficiency virus
HPLC	high performance liquid chromatography
ICM	inner cell mass
iPS	induced pluripotent state
JARID	Jumonji/AT-rich interactive domain
JHDM	Jumonji C-containing histone demethylases

JmjC	Jumonji C
KAT	lysine acetyltransferase
KDM5b	lysine demethylase 5b
KMT	lysine methyltransferase
LIF	leukemia inhibitory factor
LSD1	lysine specific demethylase 1
MALDI-MS	matrix-assisted laser desorption/ionization mass spectrometry
MRM-MS	multiple reaction monitoring mass spectrometry
NeuroD2	neurogenic differentiation factor 2
NF	neural filament
PCNA	proliferating cell nuclear antigen
qPCR	quantitative polymerase chain reaction
REST	repressor element 1-silencing transcription
Sox	sex determining region Y
SYN	synapsin
TCF3	transcription factor 3
TRAIL	tumor necrosis factor-related apoptosis-inducing ligand
TSS	transcriptional start site
TUJ1	neuron-specific class III beta-tubulin
UTR	untranslated region

Chapter 1

1 Literature Review

1.1 Embryonic stem cell model

The ability of a single-cell zygote to generate all specialized cell types of an organism introduces the remarkable potential of embryonic stem cells. At the pre-implantation blastocyst stage of development, there exists two cell lineages. A layer of epithelial cells form the trophectoterderm, a lineage contributing to the fetal placenta (Tanaka et al 1998). Encapsulated in the trophectoderm is the pluripotent inner cell mass (ICM), an aggregate of cells capable of forming any differentiated cell type of the developed organism. The inner cell mass progresses into three separate layers, the ectoderm, mesoderm, and endoderm. Cells of the outer later form structures of the ectoderm lineage, including skin, hair, tooth enamel, and the nervous system. The inner layer, the endoderm, gives rise to internal organs such as the heart, lungs, and stomach. Between these layers is the mesoderm, which will generate muscle, bones, connective tissues, kidneys, and the circulatory system (Kessler and Melton 1994, Martin 1981).

The pluripotent properties of cells in the mouse ICM have been successfully maintained *in vitro* as cultures of embryonic stem cells (ESCs) (Evans and Kauffman 1981). These cells retain their self-renewing capabilities when leukemia inhibitory factor (LIF) is introduced into the media, allowing for feeder-independent proliferation (Williams et al 1988). In relevance to our study, ESCs can differentiate into neurons with the removal of LIF and the aggregation of cells on nonadherent plates. When aggregates are transferred back to adherent plates, neural outgrowths form and differentiated cells can continue to propagate. The successful culture of ESCs has provided a suitable model to investigate how mammals develop *in utero*, and has also introduced possibilities of cell replacement therapy and tissue regeneration. Not only have ESCs contributed to our understanding of developmental disorders, stem cell therapy has further been implicated in cardiac repair, Parkinson's disease, diabetes, and in the treatment of cancer (Thomson et al 1998).

1.2 Maintenance of pluripotency

Takahashi and Yamanaka in 2006 revealed the reprogramming of adult cells into an embryonic-like state. A set of four factors introduced into mouse fibroblasts reverted the adult cells into an induced pluripotent stem (iPS) state. iPS cells expressing Oct4, Sox2, c-Myc, and Klf4 displayed stem cell markers, were morphologically identical to ES cells, and contributed to mouse embryonic development. iPS cells provide a promising outlook for regenerative therapy, circumventing the issue of tissue rejection following transplantation in patients.

Many factors have been characterized in embryonic stem cells, perhaps the most well known being Oct4. Mammalian POU transcription factor Oct4 is expressed only in early embryos and germ cells, and is imperative for the maintenance of self-renewal (Nichols et al 1998). In the mouse blastocyst, Oct4 expression is present in the ICM but not in the trophectoderm (Palmieri et al 1994). *In vitro,* Oct4 is expressed in ESCs, as well as embryonal carcinoma and embryonic germ cells (Okamoto et al 1990, Rosner et al 1990). Reduction of Oct4 expression in mouse embryos promoted differentiation of ICM cells into trophectoderm, while increasing expression promoted endoderm differentiation (Niwa et al 2000). As a master regulator of pluripotency, Oct4 is under constant control to ensure the correct levels of developmental factors and the proper growth of the embryo. Oct4 regulates a variety of other genes by direct activation or suppression, or through dimerization with other factors (Pan et al 2002, Pesce and Scholer 2001). Oct4 transrepression of human chorionic gonadotropin (hCG) genes may be the first step toward trophectoderm lineage (Liu and Roberts 1996). Oct4 regulation is further evident in binding with the zinc-finger transcription factor Rex-1, and in the activation of fibroblast growth factor FGF4 through interaction with Sox-2 (Ben-shun et al 1998, Curatola and Basilico 1990).

While Takahashi and Yamanaka's iPS cells were most successful when all 4 factors were introduced, it was subsequently shown that c-Myc and Klf4 were dispensable (Nakagawa et al 2008). However, studies indicate that Oct4 and Sox2 are necessary for the maintenance of pluripotency in human and mouse stem cells (Huangfu et al 2008). In a separate study, Oct4 and Sox2 induced pluripotency in human somatic cells in conjunction with stem cell factors Nanog and Lin28 (Yu et al 2007). Oct4 and Sox2 are appear to play

important roles in stem cell maintenance, while Oct4 and Nanog have been recognized to interact as masters of stem cell transcription. The omeodomain protein Nanog is expressed in pluripotent cells and works to maintain self-renewal through suppression of cell differentiation (Torres and Watt 2008). Each of these stem cell factors work collaboratively to ensure a precise state of transcriptional regulation. Oct4, Sox2 and Nanog regulate many of the same target genes and are found to co-localize at these regions.(Luo et al 2008). With their binding sites in close proximity, stem cell factors form a self-reinforcing network that promotes expression of renewal genes while repressing genes involved in differentiation. Such stringent orchestration of pluripotency enables ES cells to perpetuate stem cell qualities and maintain the integrity of the developing embryo.

1.3 Cell cycle control in cancer and development

Most cells in the body reside in an out-of-cycle state, while a minority are actively proliferating. Cells in active cycling are located primarily within self-renewing tissues such as epithelia and bone marrow. The majority of cells have irreversibly withdrawn from the division cycle into either a terminally differentiated lineage or into quiescent G_0 state (Williams and Stoeber 2011). Progression through each phase of the cell cycle relies on the mechanisms of cyclin-dependent kinases (CDKs) to ensure the correct transition of events. In an occurrence of aberrance such as DNA damage, CDK inhibitors are able to temporarily halt progression so that the cell cycle system can be repaired. In tumorigenesis, deregulation of the cell cycle machinery occurs, resulting in uncontrolled proliferation and a malignant phenotype. The invasive growth of cells characteristic in cancers is linked to a reduction in sensitivity to signals that control the cell cycle. Normal signaling mechanisms allow cells to respond and carry out events such as migration, differentiation, or apoptosis (Collins et al 1997). The onset of cancer may result from the presence of oncogenes that promote proliferation factors, or from the mutations of tumor suppressor genes that regulate cell cycle progression (Aaronson 1991, Weinberg 1991). It is established that several cancers accompany the mutation of retinoblastoma (Rb) protein (Horowitz et al 1990). Rb is normally found in an underphosophrylated state preceeding G_1 phase until checkpoints allow for phosphorylation and functional inactivation (Weinberg 1995). Thus, conditions that

favour Rb phosphorylation support cell proliferation through the activity of E2F genes (Figure 1.1). It is no surprise that a mutation in Rb results in a loss of proliferative control and the onset of a malignant phenotype.

In order for cells to undergo arrest and terminally differentiate, it is necessary to block the cell cycle either by downregulating cyclins or by activating CDK inhibitors. For example, mice lacking the CDK inhibitors p21 and p27kip1 are unable to form many cell types during embryonic development, a direct result of failure to exit cell cycle (Zhang et al 1999). Inhibition of cyclins can promote differentiation through the action of Rb and the basic helix-loop-helix (bHLH) transcriptional activation of lineage-associated genes (Figure 1.1). Certain factors involved in cell cycle withdrawal often carry dual roles in differentiation and cancer. Early growth response protein 1 (Egr1) is induced immediately during differentiation and increases in expression as cells terminate into cardiac and neural lineages (Sukhatme et al 1988, Lanoix et al 1998). Its role in cell cycle includes responding to stress signals, regulating proliferation, and mediating apoptosis (Liu et al 1998). Egr1 also performs paradoxical functions in tumor suppression as well as progression, and has become a relevant target for cancer therapy (Gitenay et al 2010). This factor is one of many that provide a link in cell cycle proliferation versus differentiation. Many effectors that are involved with cell cycle control and lineage determination are also implicated in cancer studies due to improper regulation of proliferation. In understanding normal and aberrant checkpoint control, studies continue to reveal multifaceted roles for factors involved in development.

Figure 1.1 Cell cycle control genes regulate proliferation versus differentiation

Prior to each mitotic division, cells must undergo a series of checkpoints governed by cyclins and CDKs. Through this process, ESCs can then decide to progress into cell cycle and continue to proliferate, or exit the cycle and begin transcription of differentiation genes. Several cancers arise from a mutation of retinoblastoma (Rb), a pivotal regulator of differentiation and proliferation. Phosphorylation inactivates Rb and promotes cell cycle progression through the activation of E2Fs; a mutation in Rb supports the loss of proliferative control. When conditions allow for cell cycle exit, Rb promotes differentiation by inactivating E2F genes and at the same time, by relieving inhibition of bHLH transcription factors that allow expression of lineage-specific genes.

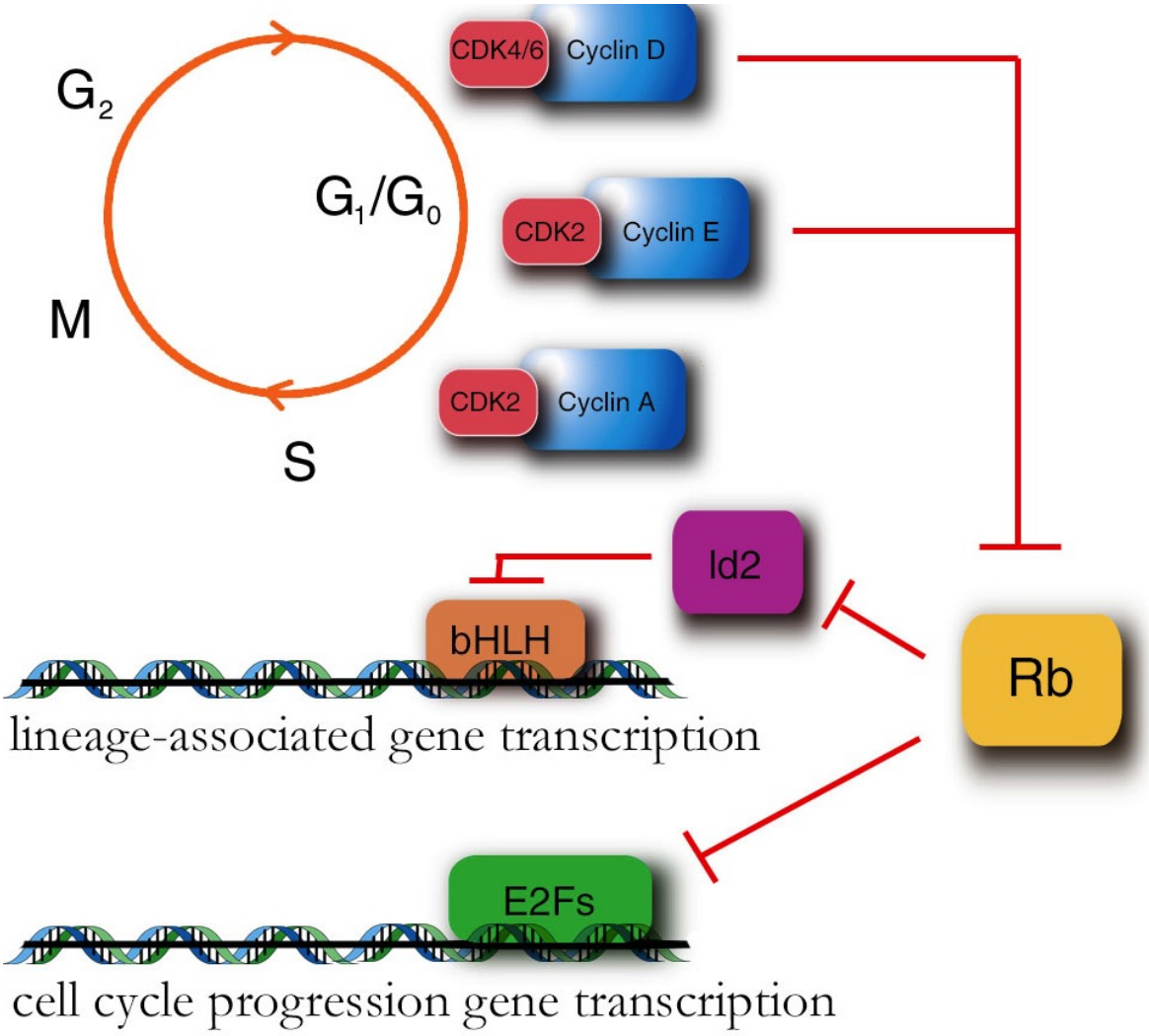
G2
G1/G0
M
S
CDK4/6
Cyclin D
CDK2
Cyclin E
CDK2
Cyclin A
Id2
bHLH
lineage-associated gene transcription
Rb
E2Fs
cell cycle progression gene transcription

1.4 Epigenetic gene regulation

The last decade of genetic research has shifted focus to the role of epigenetic mechanisms in governing cell fate decisions. Since all specialized cells of an organism arise from a single-cell zygote, variation in gene expression is attributed to differences at the epigenetic level. Wu and Morris (2001) describe epigenetics as change in heritable gene function that does not entail a change in the primary DNA sequence. DNA methylation is essential for embryonic development and plays a role in gene expression, X chromosome inactivation, genomic imprinting, silencing retroviruses, and has also been implicated in the progression of cancers (Jahner et al 1982, Jones and Laird 1999). The first wave of DNA demethylation occurs during preimplantation and serves to eliminate much of the inherited parental methylation pattern. Following implantation, the embryo then experiences *de novo* methylation, establishing the new embryonic methylation pattern (Monk et al 1987). The DNA methyltransferase activity of early embryos is attributed to members of the Dnmt2 and Dnmt3 families; subset genes *Dnmt3a* and *Dnmt3b* are highly expressed in undifferentiated ES cells and are required for the genome-wide *de novo* methylation essential for mammalian development (Okano et al 1998). High GC content areas called CpG islands are often found in promoter regions of tissue-specific genes and are differentially methylated to create specific methylation profiles for each tissue type (Shiota et al 2002). Hattori et al in 2004 demonstrated that Dnmt3a and Dnmt3b are required for DNA methylation at these tissue-specific regions and are important in the maintenance and de novo methylation of CpG islands in ES cells.

While epigenetics encompasses the study of DNA methylation, much study focuses on the diversity of covalent histone modifications. In the nucleus, histones H2A, H2B, H3, and H4 associate with histone H1 and linker DNA, assembling into high order chromatin (Luo and Dean 1999). Such tight packaging of chromatin consequently inhibits access of DNA-binding proteins to promoter regions (Suman et al 1994). However, chromatin structure can undergo remodeling via the activity of post-translational modifications such as ubiquitination, acetylation, methylation, or phosphorylation, collectively forming the "histone code" (Davie 1998). These enzyme-specific modifications occur on amino acid residues exposed on histone tails, stimulating chromatin structural changes and inducing

repression or activation of target genes. Almost all of the histone modifications have been shown to be reversible; their implementation and removal contribute to many processes including replication, repair, recombination, transcription and RNA processing.

1.5 The Histone Code

Of the known post-translational modifications, histone acetylation has been the most studied. Acetylation is a reversible mark mediated by acetyltransferases (HATs) and deacetyltransferases (HDACs), transferring an acetyl group to the N-terminal tails of histone lysine groups. These post-translation modifications play multiple roles in transcriptional regulation during cellular processes, supporting the recruitment of transcription factors and RNA polymerases to gene promoter regions (Struhl 1998). The presence of acetylated lysine alters chromatin structure toward a relaxed state and allows for the binding of transcriptional activators or repressors. On the other hand, deacetylation supports gene silencing and a more restricted state of chromatin (Deckert and Struhl 2001).

Another actively studied modification focuses on phosphorylation of residues in histones H1 and H3. In particular, phosphorylation of Histone 3 Serine 10 emerged as an important mark in transcriptional activation as well in chromosomal condensation during mitosis (Cheung et al 2000). Furthermore, histone phosphorylation has also been implicated in the induction of early mammalian genes such as the *c-Fos* gene (Mahadevan et al 1991).

Other histone modifications that are less studied include ubiquitination, sumoylation, and methylation. The two types of histone methylation occur on either arginine or lysine residues. Arginine methylation is involved in gene activation, RNA metabolism, and DNA damage repair (Bedford and Richard 2005). For the purpose of our investigation, we focus our study on the methylation of histone lysine residues. Five lysines on histone H3 (K4, K9, K27, K36 and K79) as well as one lysine on histone H4 (K20) have demonstrated methylation via specific lysine-targeted enzymes (Sims et al 2003). Continual effort in expanding the histone code will provide new insights into chromatin remodeling and the role of post-translational modifications in human development and disease.

1.6 Lysine methylation and chromatin remodeling

Histones can be methylated on their arginine or lysine residues through the action of a lysine methyltransferase (KMT). Histone lysine methylation can occur in mono-, di-, or trimethylated states and are catalyzed either by the same enzyme or a set of different enzymes. The reaction can either result in active transcription by RNA polymerase II or transcriptional repression through heterochromatization (Shilatifard 2008). For example, Histone H3 Lysine 4 methylation is a hallmark of actively transcribed genes conserved in a variety of organisms. This site is subject to mono-, di-, and trimethylation via the COMPASS methylase complex, which includes Set1 lysine methyltransferase (Schneider et al 2005). Although the function of H3K4 me1 and me2 marks remain elusive, H3K4me3 is known to activate transcriptional initiation, elongation, and RNA processing in higher eukaryotes. Similarly, the function of H3K36 methylation has also been elucidated as a mark of active chromatin. In higher eukaryotes, it is believed that the three methylation events of H3K36 are catalyzed by separate mono-, di-, and trimethylases (Lee and Shilatifard, 2007). The SET domain-containing trimethylase Set2 interacts with the large subunit of RNA polymerase II, again stimulating active gene transcription (Kizer et al 2005).

On the contrary, H3K27 methylation is an established mark of gene repression and is mediated by EZH2, a component of the Polycomb PRC2 complex. Originally identified as a Hox gene repressor, the PRC2 complex is also involved in X chromosome inactivation, cell cycle regulation, cancer, and stem cell identity (Tomek and Wysocka 2007). The presence of H3K27me3 recruits and stabilizes Polycomb PRC1 complex on chromatin, subsequently resulting in gene silencing (Schuettengruber et al 2007). An additional mark of histone repression occurs on Histone 3 Lysine 9 and represents a hallmark of constitutive heterochromatin. The associated lysine methyltransferase G9a recognizes Histone 3 Lysine 9 through its SET domain, resulting in trimylation of the histone and recruitment of heterochromatin protein 1 (Krishnan et al 2011). This silencing mechanism is evident on many genes such as Oct4, Nanog, and Dnmt3L, all closely involved in maintaining the ESC phenotype (Epsztejn-Litman et al 2008). The G9a-mediated heterochromatization of Oct4 confers a condensed “closed” state of genetic material involving the association of several

chromatin factors (Melcer and Meshorer 2010). Such key genes are regulated at the epigenetic level to reiterate the importance of controlled expression levels in development.

An interesting revelation of chromatin dynamics involved the presence of both active and repressive histone marks on the promoters of both mouse and human embryonic stem cells. It was revealed through genomic analyses that the presence of H3K27me3 repressed expression even at target genes containing high levels of H3K4me3, a mark of active transcription. Regions containing both active and repressive marks have been termed “bivalent domains” and are often found in ES cells at promoters of genes encoding key developmental transcription factors (Bernstein et al 2007). The repressive H3K27me3 mark is considered dominant over the activating H3K4me3 mark, maintaining genes in a repressed mode. However, their promoters are bound by RNA Polymerase II and are held in a poised state in preparation for transcriptional elongation once the H3K27me3 mark dissociates (Herz et al 2009). Bernstein et al in 2006 revealed that about 50% of bivalent domains in ES cells coincide with the binding sites of Nanog, Oct4, or Sox2. Many of the downstream target genes bivalently colocalized were also in a repressed state, suggesting that Nanog, Oct4, and Sox2 maintain these genes in a poised state. The discovery of bivalent domains formed an additional layer of transcriptional control, contributing to our knowledge the role of epigenetic regulation in stem cell dynamics.

1.7 Histone lysine demethylases

While lysine methyltransferases are responsible for the addition of methyl groups to histone tails, the reverse process of removing these marks demands the action of an opposing enzyme. It was not until 2004 when Shi et al identified Lysine Specific Demethylase 1 (LSD1/KDM1A) as the enzyme demethylating H3K4me1/2 in fission yeast. The mammalian counterpart was isolated as part of a complex mediated by repressor element 1-silencing transcription (REST), a factor associated with regulating neuronal genes. Since methylation of H3K4 is a gene-activating mark, KDM1A contributes to the transcriptional repression of neuronal genes through the removal of this modification (Fomeris et al 2009). The function of KDM1A repression was then extrapolated to other events such as cell differentiation and tumorigenesis (Saleque et al 2007, Wang et al 2007).

There are now two known classes of histone demethylases. Those of the KDM1 family function as FAD-dependent amine oxidases and only act on mono- and dimethylated lysines (Fomeris et al 2009). The Jumonji C (JmjC) domain-containing histone demethylases (JHDMs) are Fe(II) and 2-oxoglutarate-dependent enzymes and are able to act on all three degrees of methylation (Hou and Yu 2010). The *Jumonji* (*jmj*) gene was originally identified in a mouse gene trap approach, named for the morphology of abnormal "cruciform" shape of neural plates in *jmj* mutant mice (Takeuchi et al 1995). *Jmj* is highly expressed in mouse and human embryonic stem cells and jumonji family proteins are involved in transcription and chromatin function. The JmjC histone demethylases are categorized into several groups according to sequence similarities and different groups target specific histone lysines at various states of methylation (Mosammaparast and Shi 2010). Tsukada et al (2006) purified the founding member of JHDMs, KDM2A/JHDM1, and identified the enzyme as an H3K36me1/2 demethylase. Since this discovery, thirty JmjC domain-containing proteins have been identified in mammals and are clustered into seven subfamilies: JHDM1, JHDM2, JHDM3/JMJD2, JARID, PHF2/PHF8, UTX/UTY, and JmjC domain only (Klose et al 2006).

The JARID family of proteins encompasses the two subgroups JARID1 and JARID2. While we have mentioned JmjC-containing JUMONJI/JARID2 and its role in mouse organogenesis, JARID1 has a much broader scope of function. JARID1 family proteins contain five evolutionarily conserved domains: JmjN, ARID, JmjC, PHD, and a zinc-finger domain (Figure 1.2A). The PHD domain is capable of binding methylated residues and can recruit other proteins such as HDACs to the reaction site (Chi et al 2010). As a lysine demethylase, JmjC domain forms the enzymatically-active pocket by folding into a structure of eight β-sheets. Residues within the JmjC domain bind the Fe(II) cofactor and α-ketoglutarate, producing a highly reactive oxoferryl species that hydroxlates the methylation site and eliminates the methyl group as formaldehylde (Clifton et al 2005).

There are four JARID1 members in mammals: JARID1A/RBP2, JARID1B/KDM5b/PLU1, JARID1C/SMCX, and JARID1D/SMCY. The alternate nomenclature for each of the members demonstrates the various roles JARID proteins play; for example, JARID1A was discovered as a retinoblastoma (Rb)-binding protein and thus contributes to cell cycle control (Defeo-Jones et al 1991). Our interest lies primarily in the function of JARID1B, a multifaceted protein that is evolutionarily conserved among species

(Figure 1.2B). For the comprehension of our study, we will expand on its role as a lysine demethylase (KDM5b) as well as its regulation in cancer (PLU1).

Figure 1.2 Structural domains of PLU1/JARID1B/KDM5b

The histone demethylase KDM5b is identified as a member of the JARID1 family of proteins. These proteins carry five domains including the JmjN, ARID, JmjC, PHD, and zinc-finger domains as described by Chi et al (2010) (A). The PHD domain is able to recruit HDACS, while it is the JmjC domain that forms the catalytic site through a Fe(II) cofactor. There exists four JARID1 members in mammals, and domains are evolutionarily conserved within several species (Wolfram|Alpha 2012) (B).

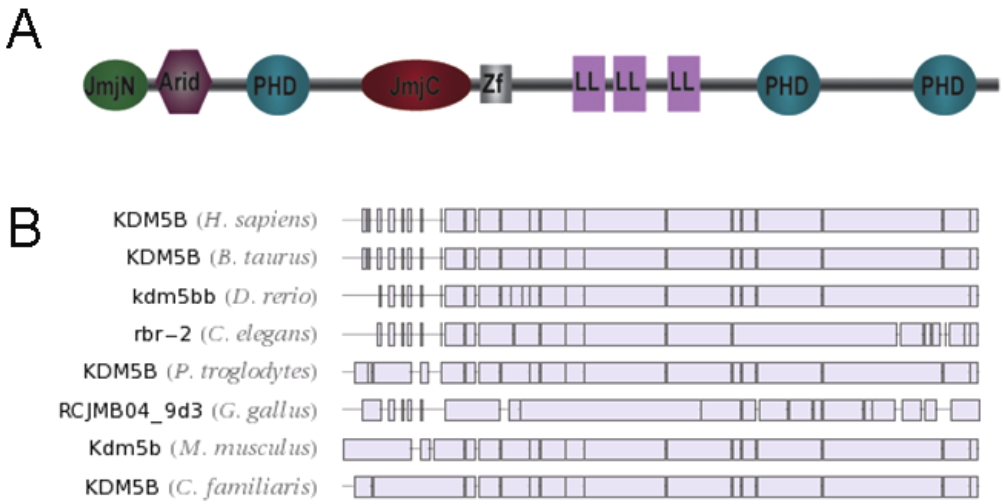
A
JmjN
Arid
PHD
JmjC
Zf
LL
LL
LL
PHD
PHD
B
KDM5B (H. sapiens)
KDM5B (B. taurus)
kdm5bb (D. rerio)
rbr-2 (C. elegans)
KDM5B (P. troglodytes)
RCJMB04_9d3 (G. gallus)
Kdm5b (M. musculus)
KDM5B (C. familiaris)

1.8 PLU1/JARID1B/KDM5b

Overexpression of the c-ErbB2 receptor is evident in breast cancers and is affiliated with poor prognosis. In a treatment experiment inhibiting this receptor, Lu et al (1999) identified PLU1 as one of the primary genes that were downregulated. PLU1 is highly expressed in breast cancer cell lines and evident in 90% of breast cancer cases; however, expression is restricted in normal adult tissues with the exception of the testis (Lu et al 1999, Barrett et al 2002). In 2006, Yamane et al recognized PLU1 as a lysine demethylase targeting H3K4me3, thus the adapted name KDM5b. The KDM5b-mediated demethylation of H3K4me3 acts to inhibit many tumor suppressor genes, including the breast cancer DNA repair gene BRCA1. The study revealed that downregulating KDM5b suppressed mammary tumor growth in a mouse cancer model. The protein was additionally identified as an oncogene for prostate, lung, bladder, and skin cancers (Hayami et al 2010, Xiang et al 2007). Findings also indicate that KDM5b demethylation of H3K4 at the KAT5 promoter interferes with regulatory control and enhances the invasiveness of cancer cells (Yoshida et al 2011). Downregulating KDM5b in cancer cell lines also inhibited the transcription factors E2F1 and E2F2, two proteins involved with cell cycle control, proliferation, and tumor suppression. Since the downregulation of KDM5b mitigated tumor progression and cell proliferation, the lysine demethylase would be an ideal candidate for drug targeting therapy in many cancers.

Although initial studies of KDM5b involved tumorigenesis, its roles in cancer cell growth and control are also implicated in the developmental model. KDM5b knockout mice showed embryonic lethality and arrested at E4.5, suggesting that KDM5b is required for implantation and later stages of development (Catchpole et al 2011). This finding is in contrast with JARID1A knockout embryos which were viable and fertile. No other members of the JARID proteins were able to compensate for the loss of KDM5b expression. In a yeast two-hybrid screen, KDM5b was shown to corepress two factors critical for mouse development: BF-1, which regulates neural development, and PAX9, a factor that regulates neural crest development (Tan et al 2003). In 2011, Schmitz et al confirmed the role of KDM5b in a stem cell model, demonstrating that the demethylation of H3K4me3 occurs predominately at genes encoding developmental regulators. Nearly all gene promoters in ESCs are bound by H3K4me3, many also marked by the repressive H3K27me3 in a state of

bivalency. In the transition from self-renewal to differentiation, levels of H3K4me3 decrease and the resolution of bivalent domains occurs (Bernstein et al 2006). Depletion of KDM5b lead to global increase of H3K4me3, failed silencing of lineage genes and impaired neural differentiation of ESCs (Schmitz et al 2011). This verified that KDM5b plays an imperative role in the differentiation of cells and the development of the embryo.

Although Schmitz et al proclaim that the demethylase is dispensable for ESC self-renewal, other studies reveal the function of KDM5b in activation of pluripotent genes. Xie et al (2011) reveal KDM5b as a downstream target of Nanog and Oct4, occupying transcribed regions of genes involved with self-renewal. While verifying the function of KDM5b in demethylating H3K4me3 in ESCs, Xie et al also confirmed binding to the activating mark H3K36me3. Knockdown of KDM5b reduced pluripotency-associated genes while increasing expression of lineage-specific genes, resulting in differentiation and the loss of self-renewal. A decrease in ESC proliferation was demonstrated in conjunction with a higher percentage of cells in G_1 phase of mitosis. Consistent with this investigation, Dey et al (2008) revealed the function of KDM5b in blocking cell cycle exit when ESCs decide between proliferation and differentiation. The reduced expression was associated with the loss of H3K4me3 at the promoters of cell cycle genes. Furthermore, constitutive KDM5b in ESCs promoted the expression of progenitor markers, retained Oct4 and Nanog, and cells were unable to properly differentiate into neural lineage. Thus, Dey et al reiterate the role of KDM5b in stem cell proliferation, and in propagating ESCs in an uncommitted and self-renewing state. Our investigation strives to elucidate the consequences of KDM5b inactivation in a stem cell model, and also to examine the expression of target genes as a result of demethylase inhibition.

1.9 Histone H2B

While most of the work involving epigenetics and post-translational modification focuses on histones H3 and H4, very little is known about the transcriptional roles of histones H2A and H2B. Kao et al in 2004 established the ubiquitination of histone H2B in *Saccharomyces cerevisiae*, the only histone species known to be ubiquitinated in yeast (Robzyk et al 2000). Subsequent work identified monoubiquitination on H2B Lysine 123, a mark involved in

chromatin compaction, chromosomal segregation, and the establishment of other histone marks such as H3K4me3 and H3K79me3 (Latham et al 2011, Wang et al 2011, Schulze et al 2011). In *Neurospora crassa*, H2B histone was revealed as a target for HDACs and a regulatory component of DNA methylation as well as heterochromatin formation (Smith et al 2010). In *Drosophila melanogaster*, Maile et al (2004) uncovered the phosphorylation of H2B Serine 33 at promoters of cell cycle genes, establishing a function in the activation of cell progression and development.

Histone H2B lysine modifications remained unknown until the identification of Lysine 37 as a site of methylation. In a top-down mass spectrometry identifying post-translational modifications, Gardner et al (2011) reported dimethylation at H2BK37 in *Saccharomyces cerevisiae.* The group additionally generated an antibody specific to this mark and confirmed its existence in yeast and in higher eukaryotes. However, a novel methyltransferase for this lysine remains unresolved, as well as the functional significance of H2BK37 methylation. Other methylation events reported at histone H3 include Lysine 122 in mice, as well as Lysine 5 in humans (Barski et al 2007, Wang et al 2008).

1.10 H2BK43 demethylation via KDM5b

Collaborators from our lab performed an MRM-MS experiment whereby KDM5b demethylase activity was examined with various methylated lysines. The technique revealed H2BK43 as a novel substrate for KDM5b. While both H2Bk43me2 and me3 were recognized substrates, maximal demethylation activity was observed on H2BK43me2 (Stalker et al 2012). The presence of KDM5b is low in mouse ESCs but increases during neural differentiation until day 5 when it is again downregulated. This pattern implies an opposing trend in H2BK43me2 expression, where it is abundant in ESCs but becomes demethylated by KDM5b as cells differentiate. On day 5, cells demonstrate a sharp increase in H2BK43me2, concomitant with the decline observed in KDM5b expression. The dynamics of both H2BK43 and KDM5b over the course of neural specification illustrate their pertinent and time-sensitive roles during differentiation, a process that abandons cell cycle and pluripotent genes in order to adopt a terminal lineage. In our study, we characterize the downstream

effects of KDM5b obstruction during ESC differentiation, through the introduction of an H2BK43 inhibitor peptide.

1.11 Applications of peptide mimetic

Synthetic peptides have provided a mechanism of therapeutic targeting in a broad scope of disease models. Sitcht et al (2005) reported a 12-mer peptide that inhibits capsid particle assembly in infectious HIV-1. Another group utilized synthetic peptides derived from p21WAF1 sequence, an inhibitor of DNA replication *in vitro*. The peptides enabled researchers to deduce p21WAF1 as an inhibitor of PCNA, a factor contributing to DNA polymerase activity (Warbrick et al 1995). Furthermore, a cell-permeable peptide blocking NF-κβ was able to ameliorate inflammation in the mouse model, encouraging a possible drug targeting therapy for the blockage of inflammatory response (May et al 2000). Inhibitor peptides have since been implicated in the biotechnology industry as possible research tools. For example, IMGENEX markets synthetic peptides as a decoy to block propagation of downstream signaling pathways. The company adds to a growing portfolio of inhibitors targeted for the manipulation of signal transduction.

Vives et al (1997) were able to improve our prospects of peptide drug delivery with the introduction of a nuclear-localizing sequence. The amino acids 47-57 of HIV TAT correspond to the protein transduction domain, the region that enables the virus to infect cells through nuclear localization. Using a truncated and modified peptide sequence, Ho et al (2001) optimized the TAT protein transduction domain to form a strong amphipathic helix capable of conveying large molecules into the cell nucleus. For our study, we synthesized a 25-amino acid peptide corresponding to regions 37-49 of histone H2B, and tagged with the modified TAT sequence at the N-terminal.

It has been demonstrated that demethylation products are capable of inactivating the demethylase reaction through a negative feedback method. H3K4me0, a demethylated product of LSD1, has been shown to bind BHC80, a downstream effector of LSD1 and a component of the LSD1 complex. The recognition to H3K4me0 by BHC80 is specific to the monomethylated mark and the interaction inhibits LSD1 enzyme activity on its substrates,

such as H3K4me2 (Lan et al 2007). H3K4 demethylation can also be inhibited by targeting monoamine oxidases, a compound with close homology to LSD1 (Lee et al 2006). Our inhibitor peptide mimics the unmethylated mark of histone H2B, an end product of KDM5b demethylation. The inhibition of KDM5b thus suppresses its demethylase activity on substrates such as H2BK43 and H3K4 methylated lysines.

1.12 Hypothesis and outline

We hypothesize that an inhibition in KDM5b enzymatic activity affects target genes involved in development and upregulates neural differentiation of mouse embryonic stem cells. To investigate our hypothesis, we constructed a synthetic peptide corresponding to unmethylated amino acids 37-49 of H2BK43 with a nuclear-localizing TAT tag. In order to validate our peptide, we purified them using HPLC, verified them with mass spectroscopy, and confirmed the interaction of H2BK43me0 with KDM5b. Our peptides were introduced into mESC culture and cells were induced to differentiate following a neural lineage time-course. We assessed phenotypic changes in ESC following peptide addition and also expression patterns throughout differentiation. To study the downstream effects of this inhibition, we examined target genes of KDM5b and the enrichment of KDM5b substrates at lineage-associated genes. Our investigation uses an optimized inhibitor peptide to closely examine cell differentiation, a novel approach in studying histone post-translational modification dynamics in stem cells.

1.13 Objectives

1. Examine phenotypic changes in ESCs and during differentiation following introduction of inhibitor peptide

2. Investigate transcriptional changes in pluripotent, cell cycle, and lineage-associated genes when cells are treated with H2BK43me0 peptide

3. Characterize the interaction of our peptide with KDM5b and its effect on alternate substrates and downstream target genes

References

Aaronson SA. (1991). Growth factors and cancer. *Science* 254:1146-1153

Barrett A, Madsen B, Copier J, Lu PJ, Cooper L, Scibetta AG, Burchell J, and Taylor-Papadimitriou J. (2002). PLU-1 nuclear protein, which is upregulated in breast cancer, shows restricted expression in normal human adult tissues: a new cancer/testis antigen? *Int. J. Cancer.* 101:581–588.

Barski A, Cuddapah S, Cui K, Roh TY, Schones DE, Wang Z, Wei G, Chepelev I, and Zhao K. (2007). High- resolution profiling of histone methylations in the human genome. *Cell.* 129:823–837.

Bedford, M. T. and Richard, S. (2005). Arginine methylation an emerging regulator of protein function. *Mol. Cell.* 18:263-272.

Ben-Shushan E, Thompson JR, Gudas LJ, and Bergman Y. (1998). Rex-1, a gene encoding a transcription factor expressed in the early embryo, is regulated via Oct-3/4 and Oct-6 binding to an octamer site and a novel protein, Rex-1, binding to an adjacent site. *Mol Cell Bio.* 18:186-1878.

Bernstein B, Mikkelsen T, Xie X, Kamal M, Hueber D, Cuff J, Fry B, Meissner A, Wernig M, Plath K, Jaenish R, Wagschal A, Feil R, Schreiber S, and Lander ES. (2006). A bivalent chromatin structure marks key developmental genes in embryonic stem cells. *Cell*. 125:315-326.

Bernstein B, Meissner A, and Lander E. (2007). The mammalian epigenome. *Cell.* 128:669-681.

Catchpole S, Spencer-Dene B, Hall D, Santangelo S, Rosewell I, Guenatri M, Beatson R, Scibetta AG, Burchell JM, and Taylor-Papadimitriou J. (2011). PLU-1/JARID1B/KDM5B is required for embryonic survival and contributes to cell proliferation in the mammary gland and in ER+ breast cancer cells. *Int J Oncol* 38:1267–1277.

Cheung P, Allis CD, and Sassone-Corsi P. (2000). Signalling to chromatin through histone modifications. *Cell.* 2013:263-271.

Chi P, Allis CD, and Wang GG.(2010). Covalent histone modifications--miswritten, misinterpreted and mis-erased in human cancers. *Nat Rev Cancer.* 10:457-69.

Clifon IJ, McDonough MA, Ehrishmann D, Kershaw N, Granatino N, and Schofield C. (2005). Structural studies on 2-oxoglutarate oxygenases and related double-stranded β-helix fold proteins. *J. Inorg. Biochem.* 100:644–669.

Collins K, Jacks T, and Pavletich NP. (1997). The cell cycle and cancer. *PNAS.* 94:-2776-2778.

Curatola AM, and Basilico C. (1990). Expression of the K-fgf proto-oncogene is controlled by 3′ regulatory elements which are specific for embryonal carcinoma cells. *Mol Cell Biol.* 10:2475-2484.

Davie JR. (1998). Covalent modifications of histones: expression from chromatin templates. *Curr Opin Genet Dev.* 8:173-178.

Deckert J and Struhl K. (2001). Histone acetylation at promoters is differentially affected by specific activators and repressors. *Mol Cell.* 21:2726-2735.

Defeo-Jones D, Huang PS, Jones RE, Haskell KM, Vuocolo GA, Hanobik MG, Huber HE, and Oliff A. (1991). Cloning of cDNAs for cellular proteins that bind to the retinoblastoma gene product. *Nature*. 352:251-254.

Dey BK, Stalker L, Schnerch A, Bhatia M, Taylor-Papidimitriou J, and Wynder C. (2008.) The Histone Demethylase KDM5b/JARID1b plays a role in cell fate decisions by blocking terminal differentiation. *Mol Cell Biol,* 28:5312–5327.

Epsztejn-Litman S, Feldman N, Abu-Remaileh M, Shufaro Y, Gerson A, Ueda J, Deplus R, Fuks F, Shinkai Y, Cedar H, and Bergman Y. (2008). De novo DNA methylation promoted by G9a prevents reprogramming of embryonically silenced genes. *Nat Struct Mol Biol.* 15:1176-83.

Evans MJ, and Kaufman MH (1981). Establishment in culture of pluripotential cells from mouse embryos. *Nature* 292:154-156.

Fomeris F, Battaglioli E, Mattevi A, and Binda C. (2009). New roles of flavoproteins in molecular biology: histone demethylase LSD1 and chromatin. *FEBS Journal.* 276:4304-4312.

Galderisi U, Jori FP, and Giordano A. (2003). Cell cycle regulation and neural differentiation. *Oncogene.* 22:5208-5219.

Gardner KE, Zhou L, Parra MA, Chen X, Strahl BD. (2011). Identification of lysine 37 of histone H2B as a novel site of methylation. *PLoS One*. 6:e16244.

Gitenay D and Baron VT. (2010). Is EGR1 a potential target for prostate cancer therapy? *Future Oncol.* 5:993-1003.

Jahner D, Stuhlmann H, Stewart CL, Harbers K, Lohler J, Simon I, and Jaenisch R. (1982). De novo methylation and expression of retroviral genomes during mouse embryogenesis. *Nature*. 298:623–628.

Jones PA, and Laird PW. (1999). Cancer epigenetic comes of age. *Nat Genet.* 21:163-167.

Hattori N, Abe T, Hattori N, Suzuki M, Matsuyama T, Yoshida S, Li E, and Shiota K. (2004). Preference of DNA methyltransferases for CpG islands in mouse embryonic stem cells. *Genome Res.* 14:1733-1740.

Hayami S, Yoshimatsu M, Veerakumarasivam A, Unoki M, Iwai Y, Tsunoda T, Field HI, Kelly JD, Neal DE, Yamaue H, Ponder BA, Nakamura Y, and Hamamoto R. (2010). Overexpression of the JmjC histone demethylase KDM5B in human carcinogenesis: involvement in the proliferation of cancer cells through the E2F/RB pathway. *Mol. Cancer.* 9:59.

Herz H, Nakanishi S, and Shilatifard A. (2009). The curious case of bivalent marks. *Dev Cell*. 17:301-303.

Ho A, Schwarze SR, Mermelstein SJ, Waksman G, and Dowdy SF. (2001). Synthetic protein transduction domains: enhanced transduction potential in vitro and in vivo. *Cancer Res*. 61:474-7.

Horowitz JM, Park SH, Bogenmann E, Cheng JC, Yandell DW, Kaye FJ, Minna JD, Dryja TP, and Weinberg RA. (1990). Frequent inactivation of the retinoblastoma antioncogene is restricted to a subset of human tumor cells. *Proc. Natl. Acad. Sci*. 87:2775-2779.

Hou H, and Yu H. (2010). Structural insights into histone lysine demethylation. *Curr Opin Cell Biol.* 20: 739–748.

Huangfu D, Maehr R, Guo W, Eijkelenboom A, Snitow M, Chen AE, Melton DA.(2008). Induction of pluripotent stem cells by defined factors is greatly improved by small-molecule compounds. *Nat Biotechnol.* 26:795-7.

Kao CF, Hillyer C, Tsukada T, Henry K, Berger S, and Osley MA. (2004). Rad6 plays a role in transcriptional activation through ubiquitylation of histone H2B. *Genes Dev.* 18:184-195.

Kessler DS and Melton DA (1994). Vertebrate embryonic induction: mesodermal and neural patterning. *Science*. 266:596:604

Kizer KO, Phatnani HP, Shibata Y, Hall H, Greenleaf AL, and Strahl BD. (2005). A novel domain in Set2 mediates RNA polymerase II interaction and couples histone H3 K36 methylation with transcript elongation. *Mol Cell Biol.* 25:3305-16.

Klose RJ, Kallin EM, and Zhang Y. (2006). JmjC-domain-containing proteins and histone demethylation. *Nat. Rev. Genet.* 7:715-727.

Krishnan , S, Horowitz S, and Trievel, RC. (2011), Structure and function of Histone H3 Lysine 9 methyltransferases and demethylases. *ChemBioChem*, 12: 254–263

Lan F, Collins RE, De Cegli R, Alpatov R, Horton JR, Shi X, Gozani O, Cheng X, and Shi Y. (2007). Recognition of unmethylated histone H3 lysine 4 links BHC80 to LSD1-mediated gene repression. *Nature*. 448:718-722.

Lanoix J, Mullick A, He Y, Bravo R, and Skup D. (1998). Wild-type egr1/Krox24 promotes and dominant-negative mutants inhibit, pluripotent differentiation of p19 embryonal carcinoma cells. *Oncogene*. 7:2495-2504

Latham JA, Chosed RJ, Wang S, and Dent SY. (2011). Chromatin signaling to kinetochores: transregulation of Dam1 methylation by histone H2B ubiquitination. *Cell*. 146:709-19.

Lee JS, and Shilatifard A. (2007). A site to remember: H3K36 methylation a mark for histone deacetylation. *Mutat Res.* 618:130-134.

Lee MG, Wynder C, Schmidt DM, McCafferty DG, and Shiekhattar R. (2006). Histone H3 lysine 4 demethylation is a target of nonselective antidepressive medications. *Chem Biol*. 6:563-567.

Liu C, Rangnekar VM, Adamson E, and Mercola D. (1998). Suppression of growth and transformation and induction of apoptosis by EGR-1. *Cancer Gene Ther.* 5:3-28.

Liu L and Roberts RM. (1996). Silencing of the gene for the beta subunit of human chorionic gonadotropin by the embryonic transcription factor Oct-3/4. *J Biol Chem.* 271:16683-16689.

Loh YH, Wu Q, Chew JL, Vega VB, Zhang W, Chen X, Bourque G, George J, Leong B, Liu J, Wong KY, Sung KW, Lee CW, Zhao XD, Chiu KP, Lipovich L, Kuznetsov VA, Robson P, Stanton LW, Wei CL, Ruan Y, Lim B, and Ng HH. (2008). The Oct4 and Nanog transcription network regulates pluripotency in mouse embryonic stem cells. *Nat Genet.* 38:431–440.

Lu PJ, Sundquist K, Baeckstrom D, Poulsom R, Hanby A, Meier-Ewert S, Jones T, Mitchell M, Pitha-Rowe P, Freemont P, and Taylor-Papadimitriou J. (1999). A novel gene (PLU-1) containing highly conserved putative DNA/chromatin binding motifs is specifically up-regulated in breast cancer. *J. Biol. Chem.* 274:15633–15645.

Luo R, Dean D (1999) Chromatin remodeling and transcriptional regulation. *Natl Cancer Inst.* 91:1288-1294.

Mahadevan LC, Willis AC, and Barratt MJ. (1991). Rapid histone H3 phosphorylation in response to growth factors, phorbol esters, okadaic acid, and protein synthesis inhibitors. *Cell*. 65:775–783.

Maile T, Kwoczynski S, Katzenberger RJ, Wassarman DA, Sauer F. (2004). TAF1 activates transcription by phosphorylation of serine 33 in histone H2B. *Science*. 304:1010-1014.

Martin GR (1981). Isolation of a pluripotent cell line from early mouse embryos cultured in medium conditioned by teratocarcinoma stem cells. *Proc. Natl. Acad. Sci*. 78:7634–7638.

May MJ, D'Acquisto F, Madge LA, Glockner J, Pober JS, and Ghosh S. (2000). Selective Inhibition of NF-κβActivation by a Peptide That Blocks the Interaction of NEMO with the IB Kinase Complex. *Science*. 289:1550-1554.

Melser S and Meshorer E. (2010) Chromatin plasticity in pluripotent cells. *Essays Biochem.* 48:245-262.

Monk M, Boubelik M, and Lehner S. (1987). Temporal and regional changes in DNA methylation in the embryonic, extraembryonic and germ cell lineages during mouse embryo development. *Development*. 99:371–382.

Mosammaparast N, and Shi Y. (2010). Reversal of histone methylation: biochemical and molecular mechanisms of histone demethylases. *Annu. Rev. Biochem.* 79:155–179.

Nakagawa M, Koyanagi M, Tanabe K, Takahashi K, Ichisaka T, Aoi T, Okita K, Mochiduki Y, Takizawa N, and Yamanaka S. (2008). Generation of induced pluripotent stem cells without Myc from mouse and human fibroblasts. *Nat Biotechnol*. 26:101-106.

Nichols J, Zevnik B, Anastassiadis K, Niwa H, Klewe-Nebenius D, Chambers I, Scholer H, and Smith A. (1998) Formation of pluripotent stem cells in the mammalian embryo depends on the POU transcription factor Oct4. *Cell*. 95:379-391.

Niwa H, Miyazaki J, and Smith AG. (2000). Quantitative expression of Oct-3/4 defines differentiation, dedifferentiation or self-renewal of ES cells. *Nat. Genet.* 24:372-376.

Okamoto K, Okazawa H, Okuda A, Sakai M, Muramatsu M, and Hamada H. (1990). A novel octamer binding transcription factor is differentially expressed in mouse embryonic cells *Cell*. 60:461–472.

Okano M, Xie S, and Li E. (1998). Cloning and characterization of a family of novel mammalian DNA (cytosine-5) methyltransferases. *Nat. Genet*. 19:219–220.

Pan GJ, Chang ZY, Scholer HR, and Pei D. (2002). Stem cell pluripotency and transcription factor Oct4. *Cell Res.* 12:321-329.

Pesce M, and Scholer HR. (2001). Oct4: gatekeeper in the beginnings of mammalian development. *Stem Cells.* 19:271-278.

Robzyk K, Recht, J, and Osley MA. (2000). Rad6-dependent ubiquitination of histone H2B in yeast. *Science.* 287:501-504.

Rosner MH, Vigano MA, Ozato K, Timmons PM, Poirier F, Rigby P, and Staudt LM. (1990). A POU-domain transcription factor in early stem cells and germ cells of the mammalian embryo. *Nature*. 345:686–692.

Saleque S, Kim J, Rooke HM, and Orkin SH. (2007). Epigenetic regulation of hematopoietic differentiation by Gfi-1 and Gfi-1b is mediated by the cofactors CoREST and LSD1. *Mol Cell*. 27:562–572.

Schmitz S, Albert M, Malatesta M, Morey L, Johansen J, Bak M, Tommerup N, Abarrategui I, and Helin K. (2011). Jarid1b targets genes regulating development and is involved in neural differentiation. *EMBO J.* 30:4586-4600.

Schneider J, Wood A, Lee JS, Schuster R, Dueker J, Maguire C, Swanson SK, Florens L, Washburn MP, and Shilatifard A. (2005). Molecular regulation of histone H3 trimethylation by COMPASS and the regulation of gene expression. *Mol Cell*. 19:849-856.

Schuettengruber B, Chourrout D, Vervoort M, Leblanc B, and Cavalli G. (2007) Genome regulation by polycomb and trithorax proteins. *Cell*. 128:735-745.

Schulze J, Hentrich T, Nakanishi S, Gupta A, Emberly E, Shilatifard A, and Kobor MS. (2011). Splitting the task: Ubp8 and Ubp10 deubiquinate different cellular pools of H2BK123. *Genes Dev.* 25:2242-2247.

Shi Y, Lan F, Matson C, Mulligan P, Whetstine JR, Cole PA, Casero RA and Shi Y. (2004). Histone demethylation mediated by the nuclear amine oxidase homolog LSD1. *Cell*. 119:941–953.

Shilatifard A. (2008) Molecular implementation and physiological roles for histone H3 Lysine 4 (H3K4) methylation. *Cell*. 20:341-348.

Shiota K, Kogo Y, Ohgane J, Imamura T, Urano A, Nishino K, Tanaka S, and Hattori N. (2002). Epigenetic marks by DNA methylation specific to stem, germ and somatic cells in mice. *Genes Cells* 7:961-969.

Smith KM, Dobosy JR, Reifsnyder JE, Rountree MR, Anderson DC, Green GR, Selker EU. (2010). H2B- and H3-specific histone deacetylases are required for DNA methylation in Neurospora crassa. *Genetics*. 186:1207-1216.

Sims R, Kenichi Nishioka K, and Reinberg D. (2003). Histone lysine methylation: a signature for chromatin function. *Trends Genet.* 19:629–639.

Sitcht J, Humbert M, Findlow S, Bodem J, Muller B, Dietrich U, Werner J, and Krausshlich HG. (2005). A peptide inhibitor of HIV-1 assembly in vitro. *Nat Struct Mol Biol.* 12:671-677.

Stalker L, Galka M, Liu H, Keating S, Doughty ML, Truant R, Li SS, and Wynder C. (2012). KDM5b localization to target genes is regulated by a novel histone modification; H2BK43me2. Manuscript submitted for publication (copy on file with author).

Struhl K. (2998) Histone acetylation and transcriptional regulatory mechanisms. *Genes Dev.* 12:599-606.

Sukhatme VP, Cao X, Chang LC, Tsai-Morris CH, Stamenkovich D, Ferreira PCP, Cohen DR, Edwards SA, Shows TB, Curran T, Le Beau MM, Adamson ED. (1988). A zinc finger-

encoding gene coregulated with c-fos during growth and differentiation, and after cellular depolarization. *Cell*. 53:37-43.

Swigut T and Wysocka J. (2007). H3K27 demethylases, at long last. *Cell.* 131: 29-32.

Takahashi K and Yamanaka S (2006). Induction of pluripotent stem cells from mouse embryonic and adult fibroblast cultures by defined factors. *Cell.* 126:663-676.

Takeuchi T, Yamazaki Y, Katoh-Fukui Y, Tsuchiya R, Kondo S, Motoyama J, and Higashinakagawa T. (1995). Gene trap capture of a novel mouse gene, jumonji, required for neural tube formation. *Genes Dev.* 9:1211–1222.

Tan K, Shaw AL, Madsen B, Jensen K, Taylor-Papadimitriou J, and Freemont PS. (2003). Human PLU-1 Has transcriptional repression properties and interacts with the developmental transcription factors BF-1 and PAX9. *J. Biol. Chem.* 278:20507–20513.

Tanaka S, Kunath T, Hadjantonakis AK, Nagy A, and Rossant J. (1998). Promotion of trophoblast stem cell proliferation by FGF4. *Science.* 282:2072–2075.

Thomson JA, Itskovitz-Eldor J, Shapiro SS, Waknitz MA, Swiergiel JJ, Marshall VS, and Jones JA. (1998). Embryonic stem cell lines derived from human blastocysts. *Science*. 282:1145–1147.

Torres J, and Watt FM. (2008). Nanog maintains pluripotency of mouse embryonic stem cells by inhibiting NFkappaB and cooperating with Stat3. *Nat Cell Biol.* 10:194-201.

Tsukada Y, Fang J, Erdjument-Bromage H, Warren ME, Borchers CH, Tempst P, and Zhang Y. (2006). Histone demethylation by a family of JmjC domain-containing proteins. *Nature*. 439:811–816.

Vives E, Brodin P, and Lebleu B. (1997). A truncated HIV-1 Tat protein basic domain rapidly translocates through the plasma membrane and accumulates in the cell nucleus. *J Biol Chem.* 272:16010-16017.

Wang CY, Hua CY, Hsu HE, Hsu CL, Tseng HY, Wright DE, Hsu PH, Jen CH, Lin CY, Wu MY, Tsai MD, and Kao CF. (2011). The C-terminus of histone H2B is involved in chromatin

compaction specifically at telomeres, independently of its monoubiquitylation at lysine 123. *PLoS One.* 6:e22209.

Wang GG, Allis CD, and Chi P. (2007). Chromatin remodeling and cancer, part I: covalent histone modifications. *Trends Mol Med*. 13:363–372.

Wang Z, Zang C, Rosenfeld JA, Schones DE, Barski A, Cuddapah S, Cui K, Roh TY, Peng W, Zhang MQ, and Zhao K. (2008) Combinatorial patterns of histone acetylations and methylations in the human genome. *Nat Genet.* 40:897–903.

Warbrick E, Lane DP, Glover DM, and Cox LS. (1995). A small peptide inhibitor of DNA replication defines the site of interaction between the cyclin-dependent kinase inhibitor p21WAF1 and proliferating cell nuclear antigen. *Curr Biol.* 5:275-282,

Weinberg RA. (1975). The retinoblastoma protein and cell cycle control. *Cell.* 81:323-330.

Weinberg RA. (1991). Tumor suppressor genes. *Science* 254:1138-1146.

Williams, GH and Stoeber K. (2011). The cell cycle and cancer. *J Pathol.* 226:352–364.

Williams RL, Hilton DJ, Pease S, Willson TA, Stewart CL, Gearing DP, Wagner EF, Metcalf D, Nicola NA, and Gough NM. (1988). Myeloid leukaemia inhibitory factor maintains the developmental potential of embryonic stem cells. *Nature.* 336:684-687.

Wolfram Alpha LLC. 2012. Wolfram|Alpha. http://www.wolframalpha.com/ (access February 16, 2012).

Wu C and Morris JR. (2001). Genes, genetics, and epigenetics: a correspondence. *Science.* 293:1103-1105.

Xiang Y, Zhu Z, Han G, Ye X, Xu B, Peng Z, Ma Y, Yu Y, Lin H, Chen AP, and Chen CD. (2007). JARID1B is a histone H3 lysine 4 demethylase up-regulated in prostate cancer. *Proc. Natl. Acad. Sci.* 104:19226–19231.

Xie L, Pelz C, Wang W, Bashar A, Varlamova O, Shadle S, and Impey S. (2011). KDM5B regulates embryonic stem cell self-renewal and represses cryptic intragenic transcription. *EMBO J.* 30:1473-1484.

Yamane K, Tateishi K, Klose RJ, Fang J, Fabrizio LA, Erdjument-Bromage H, Taylor-Papadimitriou J, Tempst P, and Zhang Y. (2007). PLU-1 is an H3K4 demethylase involved in transcriptional repression and breast cancer cell proliferation. *Mol. Cell.* 25:801–812.

Yoshida M, Ishimura A, Terashima M, Enkhbaatar Z, Nozaki N, Satou K, and Suzuki T. (2011). PLU1 histone demethylase decreases the expression of KAT5 and enhances the invasive activity of the cells. *Biochem. J.* 437:555–564.

Yu J, Vodyanik MA, Smuga-Otto K, Antosiewicz-Bourget J, Frane JL, Tian S, Nie J, Jonsdottir GA, Ruotti V, Stewart R, Slukvin II, and Thomson JA. (2007). Induced pluripotent stem cell lines derived from human somatic cells. *Science*. 318:1917-20.

Zhang P, Wong C, Liu D, Finegold M, Harper JW, and Elledge SJ. (1999). p21(CIP1) and p57(KIP2) control muscle differentiation at the myogenin step. *Genes Dev.* 13:213-224.

Chapter 2

2 Histone lysine methylation in stem cell differentiation

2.1 Introduction

The emergence of epigenetic research has lead to our curiosity to solve "the histone code." Genetic material within the cell nucleus is highly condensed with DNA wound tightly around associated proteins, or histones (Li 1975). In this state, only the histone tails of nucleosomes are accessible, and these sequences are subject to an array of post-translational modifications (Wu et al 1986). Of particular interest to us are histone lysine methylation states and their corresponding enzymes, lysine methyltransferases and demethylases (Varier and Timmers 2011). Methylation can exist in mono-, di-, tri-, or unmethylated states, and each reaction can be facilitated by separate methylating or demethylating enzymes (Shilatifard 2008). The methylation status of lysines can infer activation or repression of transcription, and in many cases, promoter regions can carry both marks in a state of bivalency (Bernstein et al 2006). Occupancy of methylated lysines on certain developmental genes provides a highly stringent mechanism for developmental control, particularly in a bivalent state where genes are repressed but poised for timely activation (Herz et al 2009, Adamo et al 2011). Many histone lysines are involved with both differentiation and tumorigenesis due the role of target genes in cell cycle control. Regulation of cell cycle is required for cells to exit mitosis and accept a terminal lineage, as well as for the maintenance of normal proliferation (Phang-Lang et al 1989, Collins et al 1997). We focus our study on KDM5b, a known lysine demethylase characterized in developmental control. The enzyme is most recognized for its upregulation in several cancers; however, its demethylase activity has been mostly restricted to H3K4me3 (Lu et al 1999, Xiang et al 2007). Most genes in stem cells are marked by H3K4me3 and are activated by this histone. KDM5b association with this activating mark ensures proper regulation of differentiation, and the depletion of KDM5b results in failed silencing of lineage-specific genes (Schmitz et al 2011).

While we attempt to elucidate the functional relevance of each of the four histones, much speculation remains regarding Histones H2A and H2B. Previous work in *Neurospora*

crassa revealed an increase of H2BK43 dimethylation following treatment with HDAC inhibitors (Anderson et al 2010, Xiong et al 2010). We extrapolate the possibility of methylated H2B in eukaryotes through examination of the lysine mark in a stem cell model. Mouse ESCs follow a differentiation time-course upon LIF withdrawal, and express many of the pluripotent and lineage-specific factors observed in mammalian development (Tremml et al 2008). In a previous experiment, our group has identified H2BK43me2 as a novel target of KDM5b and thus we have included this lysine mark into the histone code. In normal ESCs, KDMb5 acts to demethylate H2BK43 during differentiation. The increase in KDM5b activity is accompanied by a decline in the appearance of H2BK43me2 until day 5 of differentiation (Stalker et al 2012). Our current study examines differentiation of ESCs following the treatment of cells with H2BK43 inhibitor peptide. The peptides we synthesized mimic the unmethylated lysine sequence of histone H2B and inhibit the demethylase activity of KDM5b. We attached a modified HIV TAT tag to our H2BK43 sequence in order to confer nuclear localizing properties to our peptides (Vives et al 1997, Ho et al 2001). Following purification and verification by MALDI-MS, we incubated our peptides in ESC culture and examined phenotypic changes and expression dynamics throughout the neural time-course. We hypothesized that our peptide would act as an end-product inhibitor of KDM5b and would thus out-compete affinity for alternate KDM5b substrates, including H3K4me3. The interaction of our unmethylated peptide with the lysine demethylase suggests improper regulation of downstream KDM5b targets such as cell cycle and differentiation genes. Our study aims to characterize the expression patterns of KDM5b-obstructed ESCs in order to elucidate the function of H2BK43 methylation in stem cell differentiation. This investigation will provide us with a better understanding of new lysine modifications in eukaryotes and their potential regulatory roles in embryonic development.

2.2 Methods

2.2.1 Cell culture

E14Tg mouse embryonic stem cells (mESCs) were obtained from BayGenomics and maintained in ESC medium consisting of phenol red-free Dulbecco's Modified Eagle's

Medium (Gibco) supplemented with 2mM L-glutamine (Gibco), 2mM sodium pyruvate (Gibco), 0.1mM non-essential amino acid solution (NEAA) (Gibco), 0.1mM β-mercaptoethanol (Sigma-Aldrich), 1000U/mL mouse recombinant leukemia inhibitory factor (LIF), and 10% fetal bovine serum (FBS) (Gibco). Recombinant LIF was purified from bacteria in our lab. Briefly, pGEX 2T LIF (EcoRI-EcoRI) plasmid was expanded in LB media to an OD of 1.2 and then induced with 0.1mM IPTG for 3 hours. Bacterial cultures were suspended in 12.5mL cold phosphate-buffered saline (PBS) with protease inhibitors before sonicating with Sonic Dismembrator Model 60 (Fisher Scientific) at medium setting for 10s on, 50s off for four cycles. Samples were then mixed in 1% Triton-X 100 and centrifuged 30min at10000g before incubation with 400μL of glutathione Sepharose slurry. rLIF was cleaved in 80U/mL thrombin overnight before confirmation on coomassie stained gel against BSA standard. ESC cultures were grown at 37°C in a humidified 5% CO_2 incubator and passaged every two days. On alternating days, ESCs were trypsinized using 1 x TripLE solution (Gibco) for 30 seconds at 37°C and replated onto 10cm feeder-free plates pre-coated with 0.1% gelatin (Sigma-Aldrich).

2.2.2 Differentiation assay

ESCs following a neural differentiation time-course were grown to 70-80% confluency (48 hours after passage) and replaced with neurosphere media consisting of phenol red-free DMEM with 2mM L-glutamine, 2mM sodium pyruvate, 0.1mM NEAA, 0.1mM β-mercaptoethanol, 1 x B-27 supplement (Gibco), and 1% FBS. At day 2, cells were mechanically separated from adherence by vigorous pipetting, before replating 1:2 onto 10cm bacterial Petri dishes (VWR) in neural differentiation media (neurosphere media with 5% FBS). On Day 4, neurospheres were replated 1:2 onto 10cm cell culture dishes coated in 1% gelatin for the remainder of differentiation. Adherent aggregates were capable of propagation for an addition 5-10 days. Brightfield images were visualized using a Motic AE30/31 Inverted Microscope and captured using an Infinity2 camera and Infinity Campure Imaging Software.

2.2.3 Peptide synthesis

We employed a method of Fmoc (N-(9-fluorenyl)methoxycarbonyl) peptide synthesis on TentaGel rink amide resin (Novabiochem) using a 433A Peptide Synthesizer (Applied Biosystems). Fmoc-amino acid derivatives were purchased from AnaSpec and elongation of peptide resin was carried out by 0.10mmol scale from C-terminal to N-terminal. After deprotection (50% trifluoacetic acid [TFA]/dichlormethane [DCM] [v/v]) of the Boc group of the first amino acid, the next Boc-amino acid was coupled (N,N'-dicyclohexylcarbodiimide [DCC]/N-hydroxybenzotriazole [HOBt]). Methylated amino acids were manually coupled using Fmoc-protected OH-chloride lysines (AnaSpec.). Cleavage from the resin was achieved using TFA and triisopropylsilane (TIPS) and peptides were precipitated in cold ether. H2BK43 peptide corresponded to amino acids 37-49 of endogenous H2B sequence and tagged with a modified HIV TAT sequence at the N-terminal as described by Ho et al (2001). TAT peptide followed the sequence YARAAARQARAW; sequence for H2B peptides used were YARAAARQARAWYSIYVYKVLKQVH; H3K4 peptides followed the sequence YARAAARQARAWARTKQTARKS; H3K9 was synthesized with the sequence YARAAARQARAWTKQTARKSTGGKA. Crude peptides were de-salted using Sephadex G-10 affinity chromatography beads in 5% acetic acid buffer through a 20mL packed column. Fractions were manually collected at 1min intervals between 6 and 14 minutes and analyzed by Envision 2012 Multilabel Reader (PerkinElmer) at 280nm. Samples were then vacuum centrifuged for 3h at 45°C using a Thermo UVS400 speed vacuum (ThermoScientific). Dehydrated peptides were then dissolved in double distilled H_2O and adjusted to neutral pH. Peptide solutions were introduced into cell culture at a concentration of 300μM and at 24h following cell passage.

2.2.4 HPLC purification

Crude peptides were purified by high performance liquid chromatography using a 1525 Binary HPLC Pump (Waters) at a flow rate of 4.0mL/min using a gradient elution of 5% B at 0-5min, 60% B at 35min, 100% B at 36min, 5% B at 45 min (solvent B was 90% [v/v] acetonitrile, 0.1% TFA, and solvent A was 0.1% TFA in water). UV detection was performed at 260nm and 280nm with a 2487 Dual λ Absorbance Detector (Waters), fractions were

collected using a Fraction Collector III (Waters), and then analyzed with Breeze software (Waters). Masses of collected samples were determined by matrix-assisted laser desorption/ionization (MALDI)-time of flight (TOF) mass spectrometry (MS). Purified peptides were dehydrated under speed vacuum, dissolved in water at neutral pH and cultured at 300μM.

2.2.5 MALDI-MS and Gene Ontology analysis

Synthesized peptides were analyzed using MALDI-TOF MS performed on a Micromass M@LDI system (Waters) and analyzed using MassLynx software. 1μl of peptide solution was mixed on target with 1μl of 10μg/μl αCHCA (α-cyano-4-hydroxycinnamic acid) in 30/50 (v/v) CH_3CN/1% formic acid, via the dried droplet method. Mass spectrometric spectra were obtained at a laser power of 2700 kW/cm^2. For Gene Ongoloy, total RNA was labeled and hybridized to GeneChip Mouse Gene 1.0 ST arrays (Affymetrix) according to the manufacturer's protocol and scanned on a GeneChip Scanner 3000 7G (Affymetrix), with three replicates for each sample. Gene expression data was normalized by RMA (Robust Multichip Average) method using Affy, a bioconductor package in the R programming language. Differentially expressed genes were identified using a positive false discovery rate (FDR) of 0.01 and a fold-change of 2.0. Principal component analysis was performed on all experimental groups using Partek Genomics Suite software. Gene ontology of differentially expressed genes was performed using the Database for Annotation, Visualization and Integrated Discovery (DAVID).

2.2.6 Immunocytochemistry

Slides were coated in 0.1% gelatin for the adherence of ESCs and neurospheres. Cells were washed twice in PBS and fixed in 4% paraformaldehyde for 15min at room temperature. Samples were incubated with 0.2% Triton X-100 for 20min and blocked in 1% bovine serum albumin (BSA) for 1h at room temperature. All primary antibodies were incubated overnight at 4°C in the following dilutions: anti-Oct4 (Santa Cruz), 1:200; anti-TUJ-1 (Chemicon), 1:500; anti-neural filament (Sigma-Aldrich) 1:200. Secondary antibodies (anti-mouse Alexa

488) were diluted 1:1000. Slides were stained in 1μg/ml Hoechst 33342 trihydrochloride trihydrate (Invitrogen) for 15min at room temperature in order to visualize nuclei. Images were taken with a Nikon Eclipse Ti microscope, Nikon Digital Sight DS QiMC camera, and NIS Elements V3.10 SP3 software.

2.2.7 Immunoprecipitation and Western blot

Constructs of H2B and rKDM5b, nucleosome preparations, and pull-down assays were reported previously (Dey et al 2008). Briefly, cells were washed in PBS and incubated in Buffer A (10mM Tris pH 7.9, 1.5mM $MgCl_2$. 10mM KCL, 0.5mM dithiothreitol [DTT], 0.2mM PMSF) for 5min at 4°C. Samples were centrifuged and supernatant collected in Buffer E (50mM Tris pH 7.9, 25% glycerol, 0.5mM EDTA, 5mM $MgCl_2$, 0.5mM DTT, 0.2mM PMSF). The samples were then sonicated for 12min (30s on and 30s off) using a Diagenode Bioruptor. Cells were pelleted and supernatant was used for nucleosome fractions. Pull-down experiments were accomplished using biotin-labeled peptides on nucleosome preparations containing the rKDM5b-6xHis constructs. For western blots, anti-KDM5b antibody (1:2000 dilution, Bethyl labs) was used followed by HRP-conjugated secondary antibody against mouse IgG (1:1000 dilution, BioRad). Western blot was visualized using ECL from GE Healthcare.

2.2.8 Quantitative RT-PCR

RNA was prepared using Trizol reagent (Invitrogen) and reverse transcribed using qScript cDNA Synthesis Kit (Quanta BioSciences). Samples were analyzed by a C1000 Thermal Cycler and CFX384 Real-Time system (BioRad), using FastStart SYBR Green Master Mix (Roche), and analyzed on BioRad CFX Manager 2.0 software. Amplification was achieved by 40 cycles of 95°C for 10s followed by 55°C for 10s. Potential amplification of contaminating genomic DNA was ruled out using a negative control sample of mock cDNA preparations lacking reverse transcriptase. Melt curve analyses were performed following each PCR. qPCR was performed in biological triplicate experiments and values were expressed as percentages of the control per unit of GAPDH. Primers used include: GAPDH

forward (CAT GGC CTT CCG TGT TCC TA), GAPDH reverse (CCT GCT TCA CCA CCT TCT TGA); Egr1 forward (GGG AGA GGC AGG AAA GA CAT), Egr1 reverse (TCT GAG ATCT TCC ATC TGA CC); Oct4 forward (TTG GGC TAG AGA AGG ATG TG), Oct4 reverse (GGA AAA ACT GAG TAG AGT GTG); Nanog forward (CAG CCC TGA TTC TTC TAC CAG), Nanog reverse (GAT GCG TTC ACC AGA TAG CC); BRCA1 forward (GCC TAC AGG GAA GCA CAA GGT TTA), BRCA1 reverse (CCA TTT GTA AGC TGC ATT CCC GTG); NF forward (CCA GGA AGA GCA GAC AGA GGT), NF reverse (GTT GGG AAT AGG GCT CAA TCT); neuroD2 forward (CGA AGA AAC GCA AGA TGA CC), neuroD2 reverse (GAA GTT GCC GTT GAG ACA GA); TRAIL forward (CAA CTC CGT CAG CTC GTT AGA AAG), TRAIL reverse (TTA GAC CAA CAA CTA TTT CTA GCA CT); Synapsin forward (CCG CCA GCA TGC CTT), Synapsin reverse (TGC AGC CCA ATC ACC AAA); Sox17 forward (GGA TGT AAA GGT GAA AGG CGA GGT), Sox17 reverse (ACA CCA TAA AGG CGT TCA TCG GCC).

2.2.9 Chromatin immunoprecipitation (ChIP)

ESCs were washed twice in PBS and crosslinked with 1% paraformaldehyde for 10min at 37°C. Adherent cells were scraped, washed twice with ice cold PBS, resuspended in 200μL of SDS-lysis buffer containing protease inhibitor (1% SDS, 10mM EDTA, 50mM Tris pH 8.1) and incubated for 10min at room temperature. Total volume was brought up to 2mL with ChIP dilution buffer (0.01% SDS, 1% Triton X-100, 1.2mM EDTA, 16.7mM Tris-HCl pH 8.1, 167mM NaCl) and then sonicated with a Sonic Dismembrator at medium setting for 12min (30s on and 30s off). Lysates were verified by DNA electrophoresis ethidium bromide stained agarose gel to ensure fragments of 500-1000bp in size. Samples were pre-cleared with 50μL of salmon sperm DNA (Sigma-Aldrich) protein G-agarose (50%) bead slurry (Roche) for 1h at 4°C on a Nutator. Salmon sperm DNA and protein G beads were removed by centrifugation at 3000rpm for 2min at 4°C. 100μL of supernatant was collected for input control and another 100μL for PCR standards. Aliquots were incubated overnight in 65°C water to decrosslink and were gene cleaned using Purelink PCR Purification Kit (Invitrogen). Remaining supernatant was divided equally among anti-KDM5b (1μL) antibody (Bethyl), anti-H2BK43me2 (3μL) antibody (AbCam), anti-H3K4me3 (3μL) antibody (Active Motif),

or IgG control (3μL) antibody (Santa Cruz) and incubated overnight at 4°C on a Nutator. Antibody-chromatin complexes were precipitated with 45μL of salmon sperm DNA/protein G beads, agitated for 2h at 4°C on a Nutator, and then centrifuged at 3000rpm for 4min at 4°C. The beads were washed five times in 1 x low salt immune complex wash buffer (0.1% SDS, 1%Triton X-100, 2mM EDTA, 2 mM Tris-HCl pH 8.1, 15 mM NaCl) at 4°C for 5min, 1 x high salt immune complex wash buffer (0.1% SDS, 1%Triton X-100, 2mM EDTA, 20mM Tris-HCl pH 8.1, 500mM NaCl) at 4°C for 5min, 1x LiCl immune complex wash buffer (0.25M LiCl, 1% IGEPAL-CA630 [Sigma-Aldrich], 1% deoxycholic acid sodium salt [Sigma-Aldrich], 1mM EDTA, 10mM Tris pH 8.1) at 4°C for 5min, and 2 x Tris-EDTA buffer at room temperature for 5min. Chromatin was eluted from the antibody by using 100μl of 1% SDS, 0.1M NaHCO3 for 2h at room temperature. Beads were centrifuged at 3000rpm for 1min, and then supernatant was decrosslinked at 65°C overnight before purification using a Purelink PCR Purification Kit. Purified samples were analyzed by qPCR performed on C1000 Thermal Cycler and CFX384 Real-Time systems, and using FastStart SYBR Green Master Mix. Data was analyzed using BioRad CFX Manager 2.0 and represent percentages of DNA normalized by ChIP analyses to the amount of DNA found in input. These values were then compared between control and experimental samples. Values were expressed as a result of biological triplicates. ChIP-qPCR primers used were as followed: TFC3 forward (ACA GAG CCA CGC CCC TGT C), TCF3 reverse (TGC CTG GCC CGG CCC GGC G); Egr1 TSS forward (TTC ACG TCA CTC CGG GTC CTC C), Egr1 TSS reverse (AGT TCT GCG GCG CTG GGA TCT); Egr1 TATA forward (GCC GGT CCT TCC ATA TTA GG), Egr1 TATA reverse (CAA GTT CTG CGC GCT GG).

2.2.10 Statistical analysis

Results shown are presented as mean with standard deviation of the mean. Statistical analysis was performed using Microsoft Excel. All p-values were derived using student's t-test using two-sample, equal variance, two-tailed setting. Experiments were performed in biological triplicates. Results were graphed using Prism GraphPad 5.0a software.

2.3 Results

2.3.1 Synthetic peptides exhibited nuclear localization in ESCs

We constructed a 25-amino acid length peptide mimicking unmethylated H2BK43, in order to investigate the properties of stem cell differentiation when KDM5b activity is disrupted. The inhibitor peptide corresponded to amino acids 37-49 of endogenous H2B and tagged with TAT PTD. We confirmed the sequence of our peptide using MALDI-MS (Figure 1.1A). Crude peptide samples were then separated into fractions using HPLC and confirmed peaks were collected for use in stem cell culture (Figure 1.1B). Our TAT peptides were then examined for effective nuclear translocation as described previously (Frankel and Pabo 1988, Vives et al 1997). The amino acid sequence we used ensured folding into an amphipathic alpha-helix secondary structure, where charged arginine residues line one face while hydrophobic residues line the opposite (Figure 2.1C). Incubation experiments confirmed effective nuclear transduction of TAT peptides in ESCs (Figure 2.1D). We introduced a TAT-fluorescein peptide into ESC culture and refreshed media the next day. With fluorescence microscopy, we successfully imaged the nuclear localization of TAT peptides in nearly 100% of stem cells after 24 hours of incubation

2.3.2 ESCs formed neurospheres upon LIF withdrawal and aggregation

Normally, ESCs form round colonies with clear margins, but can also take on a proliferative, adherent morphology (Figure 2.2A). Both morphologies are characteristic of pluripotent stem cells and stain positive for alkaline phosphatase. Upon LIF withdrawal, ESCs begin to aggregate while some cells experience necrosis and are lifted from culture. When further aggregated in nonadherent plates, cells form distinct, rounded neurospheres suspended in the culture media from days 3 to 4. Differentiation of peptide-treated cells followed the normal ESC timecourse (Figure 2.2B). Peptides were added to media 24h following passage and incubated in culture for 24 hours (day 0). At day 0 of differentiation, media was switched to LIF-free conditions.

Figure 2.1 H2BK43me0 inhibitor peptides were confirmed, purified, and nuclear-localized in ESCs.

Following synthesis of our 25-amino acid length sequence mimicking endogenous histone H2B, we verified the identity of our peptide using MALDI-MS (A). We performed HPLC on our crude sample and identified each peak in our purification (B). Our H2BK43me0 peptide was collected in fractions between 8.25 and 8.75 minutes. Peptides were synthesized with a modified HIV TAT sequence at the N-terminal. Secondary structure of TAT forms an alpha-helix where hydrophilic arginine residues are found on one side while hydrophobic amino acids are found on the other (C). The configuration of the alpha-helix allows for its amphipathic characteristics and enable nuclear localization of TAT-mediated peptides. A TAT-fluorescein peptide was synthesized and incubated with ESCs at a concentration of 0.5nM for 24 hours. Using fluorescence microscopy of FITC (green), a colony of ESCs was visualized to have nearly 100% nuclear uptake of the TAT peptide. Images were taken at 400x magnification. Cell nuclei were visualized with DAPI.

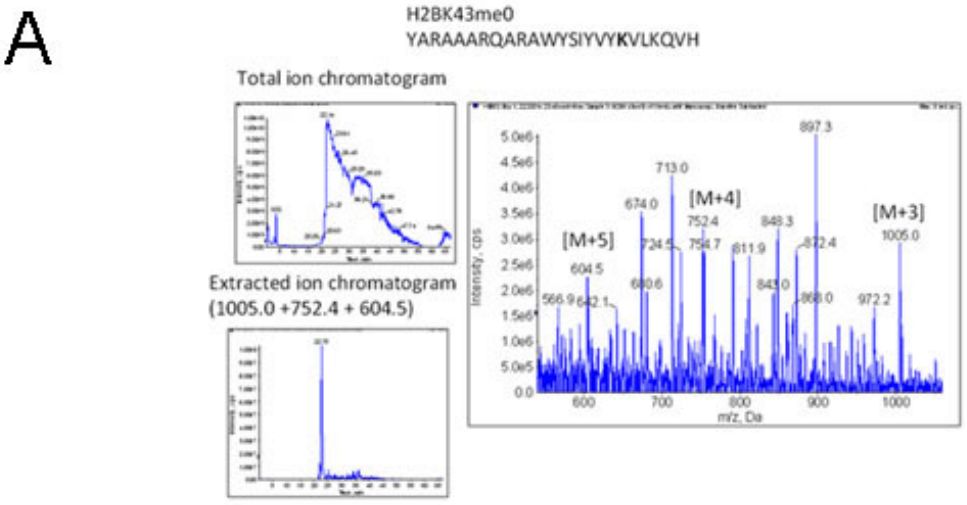
A
H2BK43me0
YARAAARQARAWYSIYVYKVLKQVH
Total ion chromatogram
Extracted ion chromatogram
(1005.0 +752.4 + 604.5)
[M+5]
[M+4]
[M+3]
Intensity, cps
m/z, Da

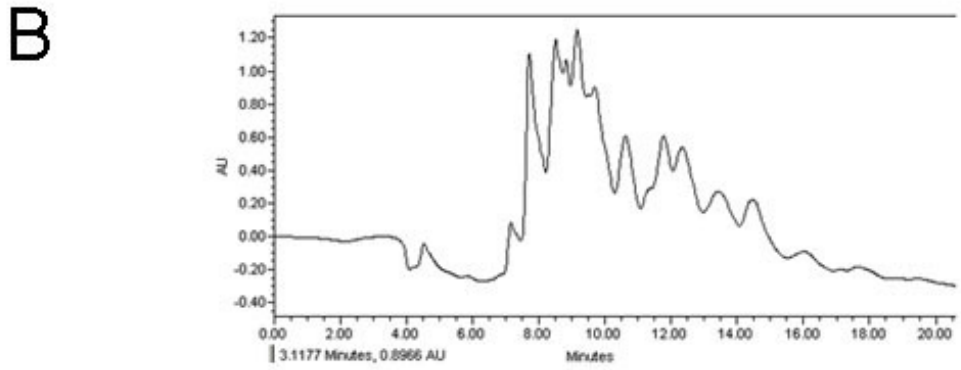
B
AU
3.1177 Minutes, 0.8966 AU
Minutes

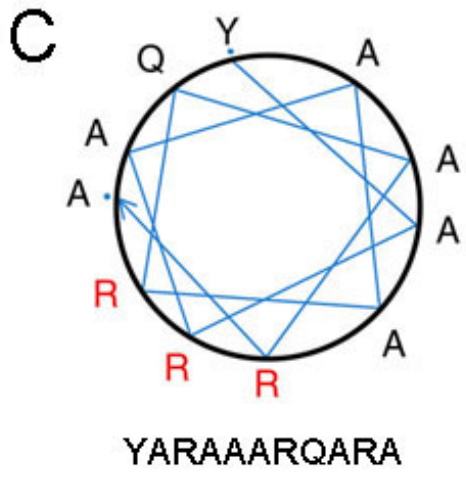
C
YARAAARQARA

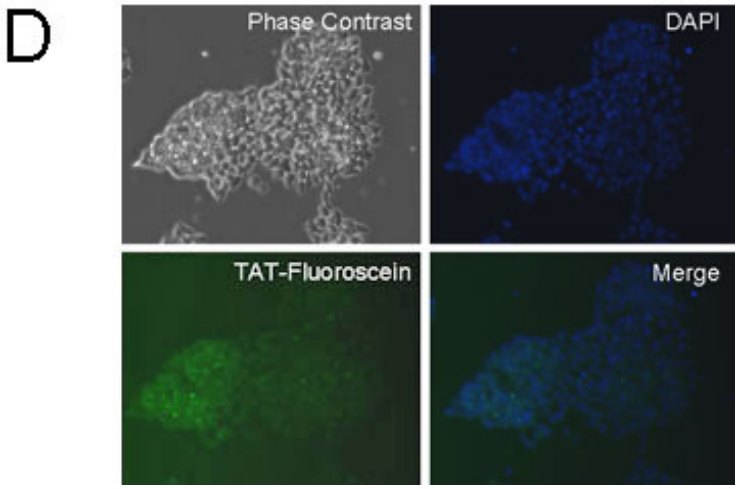
D
Phase Contrast
DAPI
TAT-Fluoroscein
Merge

Figure 2.2 Mouse embryonic stem cells begin differentiating upon LIF withdrawal and form neurospheres when aggregated

Mouse embryonic stem cells often form round colonies with defined edges, but can also adopt a spread out, proliferative morphology (A). Both ESC phenotypes are pluripotent and are positive for self-renewal markers as well as for alkaline phosphatase. Nearly 100% of cells in culture continually expressed alkaline phosphatase. On day 1 of differentiation when ESCs are serum-starved and cultured in the absence of LIF, cells start to aggregate spontaneously and many cells experience apoptosis. When cells are further aggregated on nonadherent plates, ESCs form round neurospheres. Images were obtained at 100x magnification. ESCs are differentiated following a neural time-course (B). LIF withdrawal occurs at day 0 and cells are aggregated on day 2 for 48 hours before plating on adherent cultures. When ESCs are treated, peptides are introduced into culture 24 hours following passage, incubated for 24 hours, and then removed with media change at day 0.

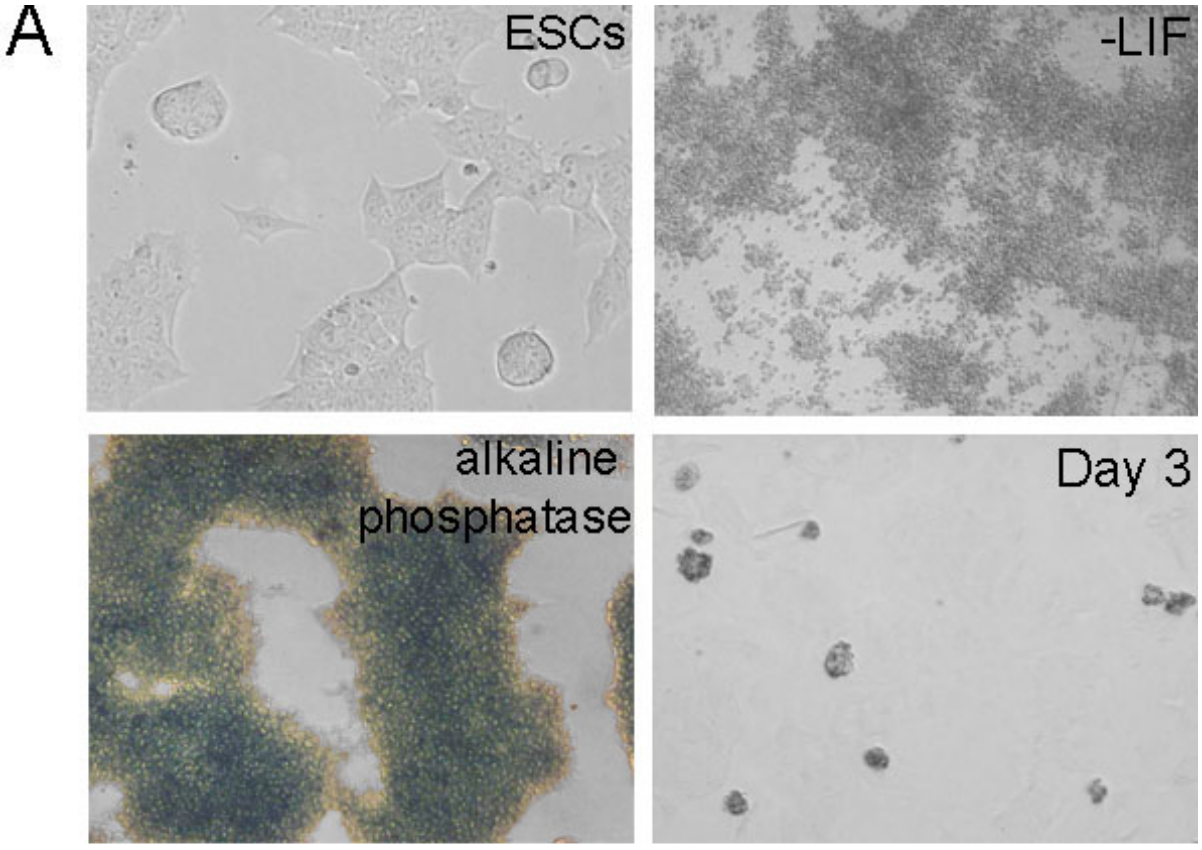
A
ESCs
-LIF
alkaline
phosphatase
Day 3

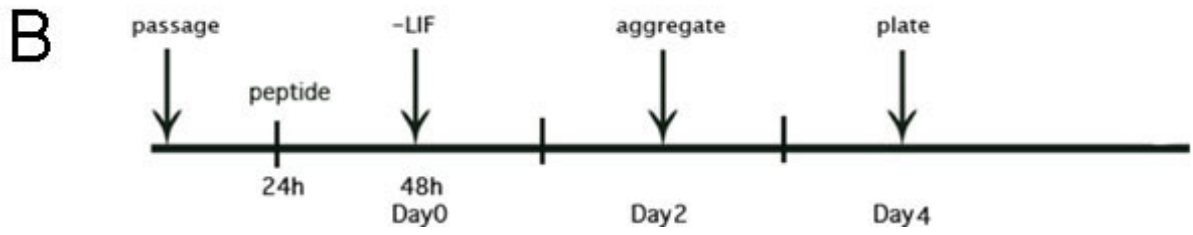
B
passage
peptide
-LIF
aggregate
plate
24h
48h
Day0
Day2
Day4

2.3.3 H2BK43 peptide promoted a neural phenotype in ESCs

Following incubation of our nuclear-penetrant inhibitor peptide, we noticed remarkable phenotypic changes in ESCs within 24 hours of treatment. While TAT-treated control cells retained pluripotent morphology, cells treated with H2BK43me0 peptide exhibited early differentiation characteristics within hours of incubation such as the initial aggregation and lifting of ESCs from culture (Figure 2.3). This phenotype is representative of early differentiation when ESCs are LIF-deprived on day 0. After 24 hours of peptide treatment, cells have further aggregated and adopt characteristic neurosphere morphologies. Aggregates of neurospheres were also found suspended in the media on the same day. At 48 hours of treatment, suspended neurospheres begin to attach to plates and we begin to see neural outgrowths and the appearance of neurons. Cells treated with TAT were unaffected and appeared as ESCs for the duration of the experiment.

2.3.4 Neural phenotype was specific to H2BK43me0 peptide treatment

In a large scale screening of 88 peptides of variable lysine methylation states, we identified H2BK43me0 as one of few peptides capable of inducing morphological transformations. Surprisingly, ESCs incubated with H2BK43me3 peptides did not promote the neural phenotype seen in the unmethylated counterpart experiment (Figure 2.4). Furthermore, when cells were treated with H3K4me0 and H3K4me3 peptides, no neural differentiation was observed and cell phenotypes were analogous to that of TAT control cells. Similarly, when we treated ESCs for each methylation state of H3K9, no changes in stem cell morphology occurred. Our treatment assays demonstrated specific induction of neural phenotype in cells treated with H2BK43me0 inhibitor peptide.

Figure 2.3 Incubating ESCs with H2BK43me0 peptide induced a neural differentiation phenotype

Within hours of peptide incubation, ESCs take on morphological changes and aggregate in culture. Treatment for 24 hours induced a neurosphere phenotype similar to embryoid bodies seen when ESCs were differentiated at day 3 of the neural time-course. Several neurospheres spontaneously became nonadherent and were suspended in the culture media. After 48 hours of treatment, many of the neurospheres developed neural outgrowths and the appearance of neurons occurred. Contrarily, cells treated with TAT control peptide did not have any observable phenotypic changes in the 48-hour duration of the experiment. ESCs were treated at 300μM peptide solution in media and images were obtained at 100x magnification.

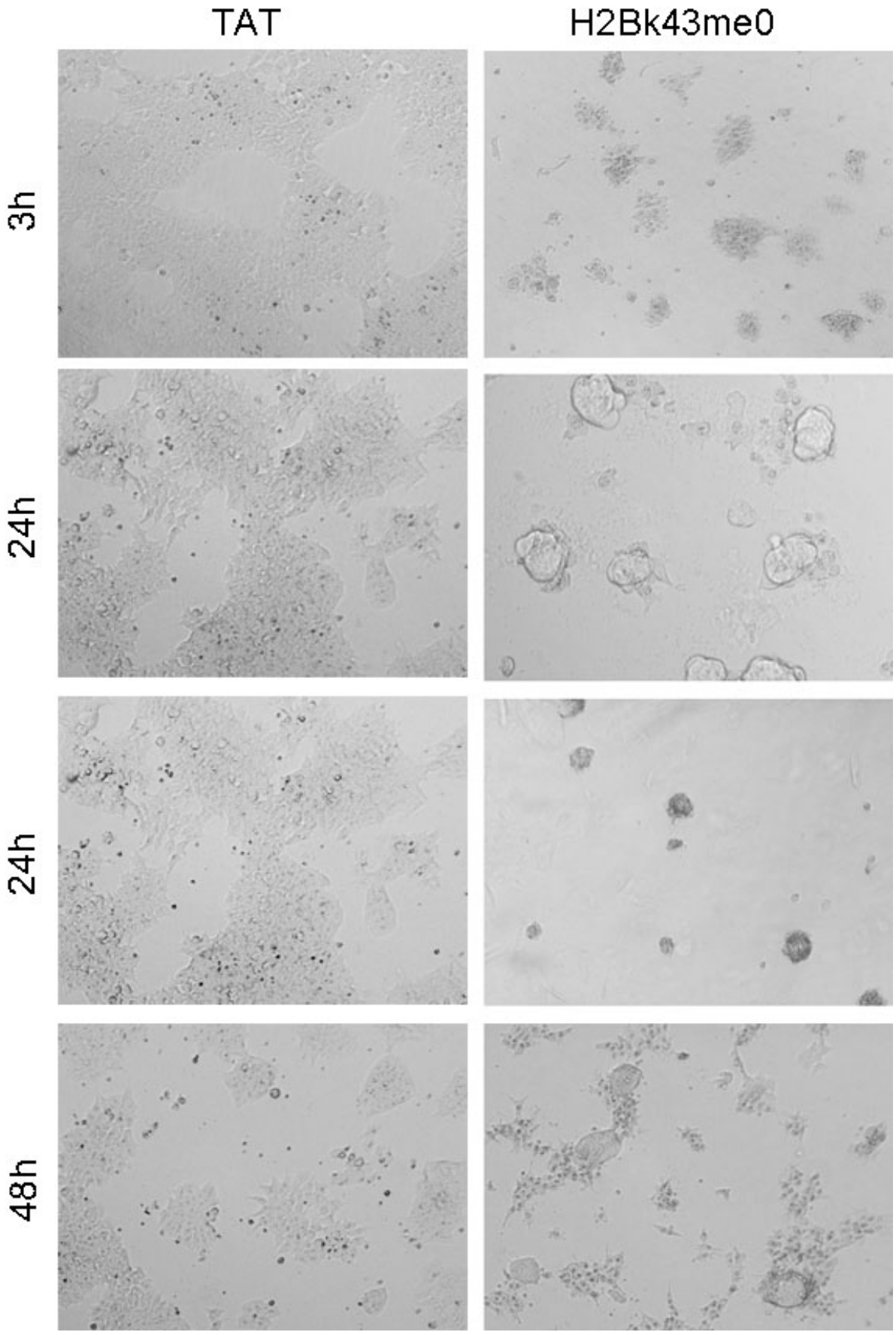
TAT
H2Bk43me0
3h
24h
24h
48h

Figure 2.4 Treatment of H2BK43me3, H3K4 and H3K9 peptides did not promote any changes in ESC morphology

When incubated with peptides corresponding to alternate methylation marks, cells retained ESC morphology and did not appear to differentiate. As an alternate to the nonmethylated lysine, we treated cells with the trimethylated counterpart H2BK43me3. Trimethylated peptide-treated ESCs appeared identical to cells treated with TAT control peptide. Similarly, when cells were treated with H3K4me0 and H3K9me0, ESCs did not aggregate in culture or demonstrate any onset of differentiation. Following treatment of H3K4me1,2,3 and H3K9me1,2,3 peptides, cell morphology was comparable to that of TAT-treated ESCs (data not shown). ESCs were treated 24 hours at 300μM peptide solution in media. Images were obtained at 100x magnification.

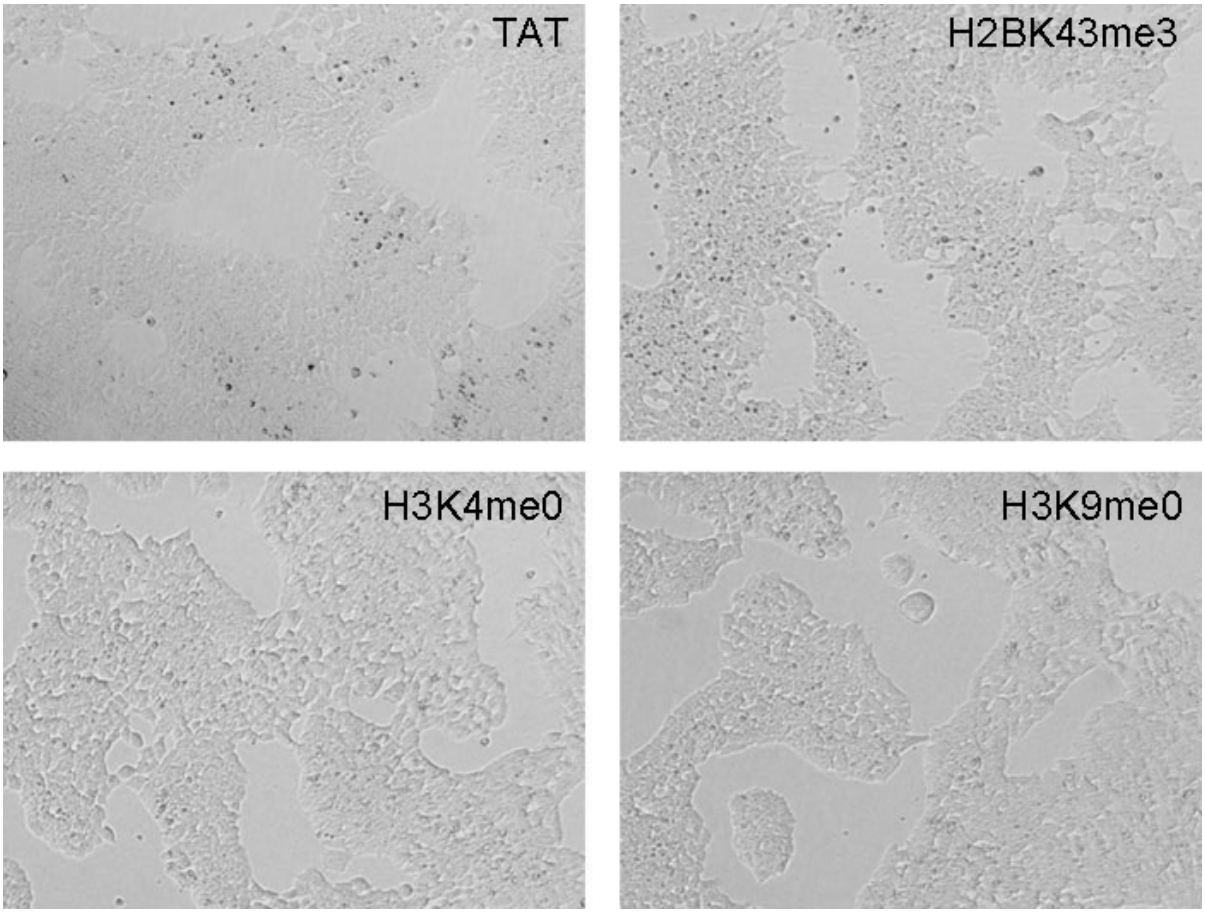
TAT
H2BK43me3
H3K4me0
H3K9me0

2.3.5 H2BK43me0 treatment downregulated pluripotency factor Nanog and induced expression of neural markers

Cells treated with H2BK43me0 peptide were assayed by qPCR for changes in pluripotent and lineage markers after 24 hours. While pluripotent marker Oct4 demonstrated insignificant changes in expression compared to TAT treatment, there was significant downregulation in expression of Nanog following peptide incubation ($p<0.05$) (Figure 2.5A). Furthermore, when ESCs were treated with H3K43me0 peptide, we observed upregulation in lineage factor, neural differentiation factor 2 (neuroD2). By comparison, TAT control cells did not amplify either NF or neuroD2 transcript. This confirmed our speculation that morphological changes in ESCs were a result of differentiation into the neural lineage. Cells cultured in peptide solution aggregated into neurospheres after 24 hours while ESCs normally do not form neurospheres until day 3 of the differentiation time-course, when cells are induced to aggregate. When we stained these cells, we observed positive expression of both NF and TUJ1 (Figure 2.5B). In contrast, ESCs treated with the TAT peptide did not express NF or TUJ1 after 48 hours. Our experiment thus verifies the onset of neural differentiation in H2BK43me0-peptide treated cells but not in our control cultures.

2.3.6 Peptide-treated ESCs upregulated expression of cell cycle gene Egr1

Following observation of a differentiating phenotype in our peptide-treated cells, we speculated an increase in expression of lineage-associated genes. Since Egr1 has been previously identified as an early gene upregulated as ESCs exit cell cycle, we expected Egr1 transcription to increase in our peptide treatment samples (Sukhatme et al 1988). We investigated the levels of Egr1 expression 48 hours following treatment, and also post-treatment at days 1 and 3 during the differentiation time-course. When cells were incubated with H2BK43me0, there was a significant increase in Egr1 transcription at day 1 ($p<0.05$), but expression was downregulated afterwards (Figure 2.6A). Since we previously did not observe morphological changes in ESCs treated with H2BK43me3 peptide, we also investigated the expression of differentiation genes in this treatment sample.

Figure 2.5 ESCs incubated with peptide inhibitor exhibited downreguation of Nanog and upregulation of neural markers

While Oct4 remained constant between TAT and H2BK43me0 treatments, there was a significant downregulation in Nanog when ESCs were incubated 24 hours with inhibitor peptide (A). Further upregulation was observed in neural markers neural filament (NF) and neuroD2. GAPDH was used as a loading control. Asterisks denote statistical significance ($p<0.05$). Experiments were run in biological triplicate ($n=3$). Bar graphs represent normalized means ± standard deviation. When we stained day 1 cells following treatment, H2BK43me0-induced neurospheres exhibited positive expression of NF and TUJ1 (green) (B). TAT cells remained pluripotent and did not stain positive for neural markers. Immunofluorescent images were taken at 400x and cell nuclei were visualized using DAPI (blue).

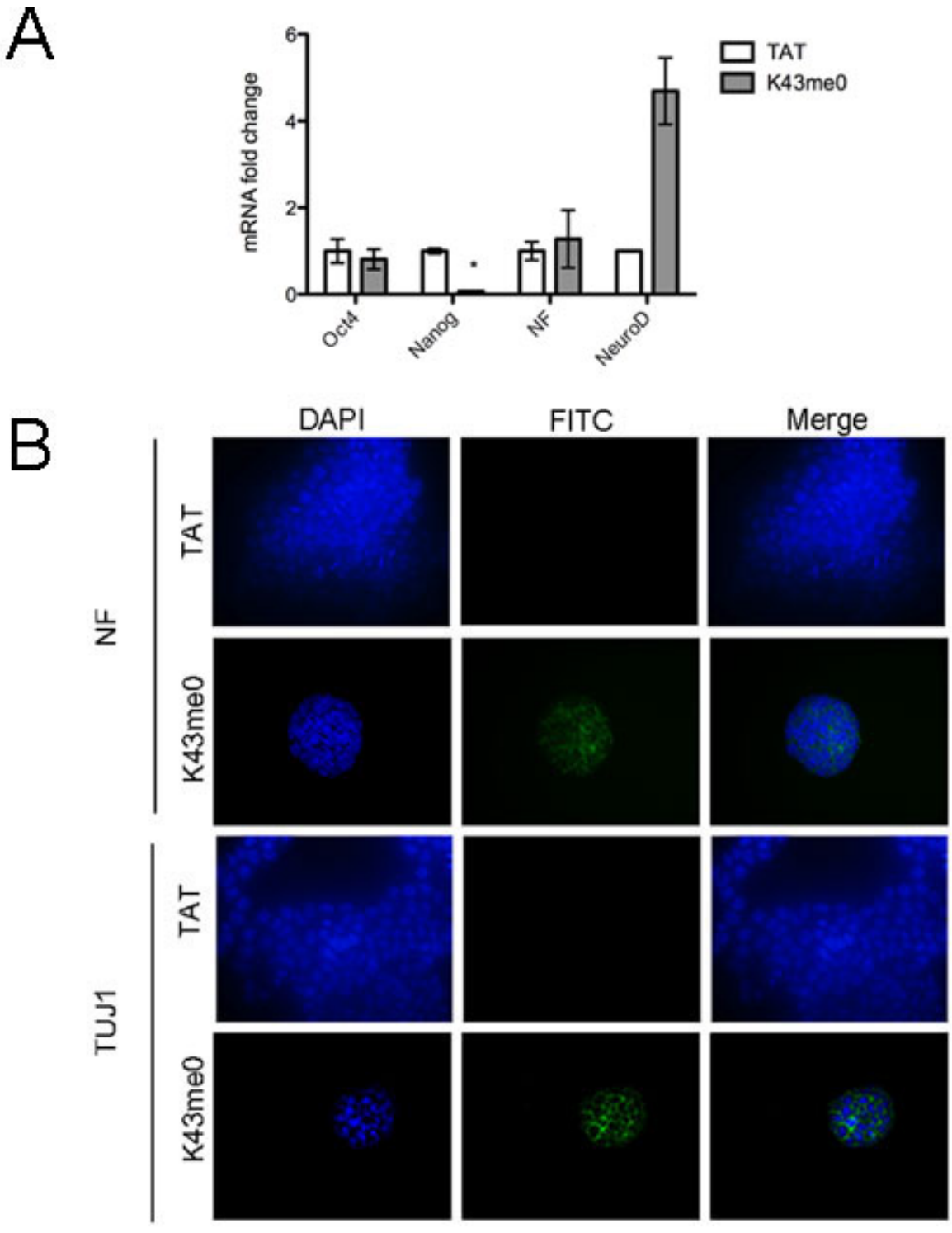
A
mRNA fold change
6
4
2
0
TAT
K43me0
Oct4
Nanog
NF
NeuroD
B
DAPI
FITC
Merge
NF
TAT
K43me0
TUJ1
TAT
K43me0

There was a similar significant upregulation in Egr1 transcript at day 1 when cells were treated with the trimethylated peptide, and a comparable downregulation at day 3. Compared to TAT, cells treated with H2BK43me0 increased Egr1 expression on each day of differentiation that we examined, with significant upregulation ($p<0.05$) at days 0 and 1. Expression of pluripotent gene Oct4 were fairly constant from days 0 to 3 in our control cells, while a significant downregulation ($p<0.05$) was observed during differentiation of our H2BK43me0-treated cells However, following day 1 of peptide treatment, Oct4 did not continue downregulation`. Furthermore, cells treated with the trimethylated peptide counterpart did not downregulate Oct4 during differentiation. Interestingly, Oct4 was still expressed on day 3 of both nonmethylated and trimethylated peptide treatments (Figure 2.6B). We stained cells treated in H2BK43me0 for 48 hours and while there was reduction of expression, Oct4 was still apparent in differentiated ESCs (Figure 2.6C). This compelled us to conclude Oct4 as a late fluctuating marker, continuing to regulate downstream genes as cells are differentiating.

2.3.7 Peptide-induced differentiation upregulated BRCA1, Synapsin, and Sox17 but not TRAIL

As a prospective KDM5b target, we examined tumor suppressor gene BRCA1 following treatment with the demethylase inhibitor peptide. BRCA1 was upregulated in expression when cells were incubated with the peptide; however, this change in expression was not observed in the treatment of H2BK43me3 (Figure 2.7A). We further examined peptide treatments of KDM5b alternate substrate H3K4. BRCA1 was significantly increased following treatment of H3K4me0 peptide ($p<0.05$). Similar patterns of upregulation were observed in the expression of both lineage-associated genes Synpasin and Sox17. (Figure 2.7B). Our experiment demonstrates the upregulation of a KDM5b target gene when the demethylase is inhibited, and confirms peptide-induced cell specification through the increase of differentiation genes. In order to eliminate the possibility of cell stress-induced differentiation, we assayed for the expression of TNF-related apoptosis-inducing ligand (TRAIL). No upregulation of TRAIL transcript was observed in any of our peptide treatment

Figure 2.6 H2BK43me0 peptide treatment resulted in the early upregulation of Egr1 compared to TAT treatment

ESCs were treated with TAT, H2BK43me0 or H2BK43me3 and induced to differentiate. Comparing the days of differentiation, H2BK43me0 peptide treatment significantly upregulated Egr1 expression on both days 0 and 1 compared to TAT (A). In contrast, Oct4 expression was relatively constant in TAT-treated cells throughout differentiation. Downregulation of Oct4 was only observed on day 1 of differentiation when cells were treated with H2BK43me0 when compared to TAT (B). GAPDH was used as a loading control. Asterisks denote statistical significance ($p<0.05$). Experiments were run in biological triplicate ($n=3$). Bar graphs represent normalized means ± standard deviation. When cells were stained for Oct4 after 48 hours of peptide incubation (green), K43me0 treatment did not demonstrate substantial decline in expression and staining remained positive in TAT control cells (C). Images were obtained at 400x magnification. Cell nuclei were visualized using DAPI.

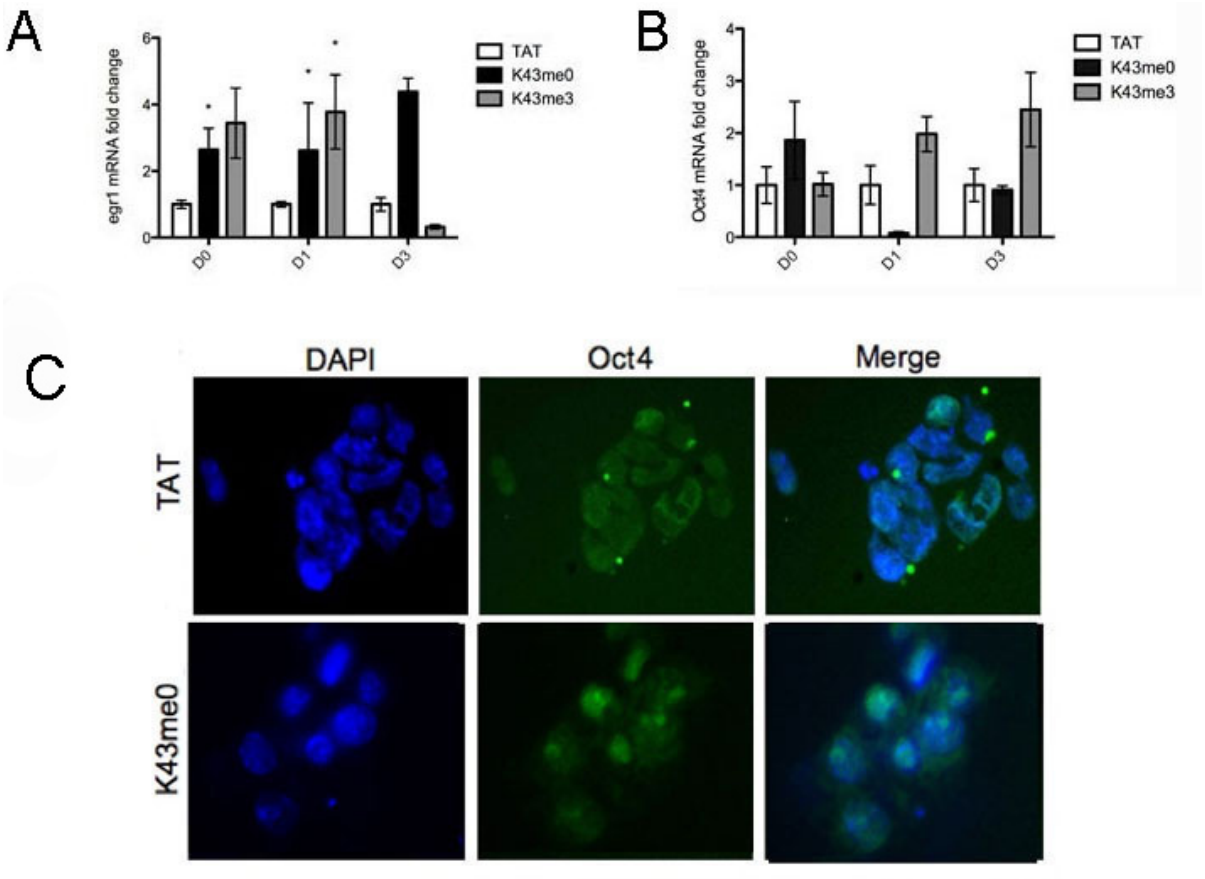
A
egr1 mRNA fold change
TAT
K43me0
K43me3
D0
D1
D3
B
Oct4 mRNA fold change
TAT
K43me0
K43me3
D0
D1
D3
C
DAPI
Oct4
Merge
TAT
K43me0

Figure 2.7 ESCs incubated with inhibitor peptide upregulated lineage genes but did not express apoptosis factor TRAIL

24-hour treatment of ESCs with H2BK43me0 peptide upregulated the expression of BRCA1, Synapsin and Sox17. Our inhibitor peptide is hypothesized to inactivate KDM5b and thus increase the expression of KDM5b target gene BRCA1. While the trimethylated peptide did not upregulate gene expression, H3K4 peptide treatments appeared to increase BRCA1, with significant upregulation in cells incubated with unmethylated H3K4 (A). The trend was also apparent in lineage-associated genes Synapsin and Sox17. Sox17 upregulation was most pronounced, with a ten fold significant increase when ESCs were treated with H2BK43me0 peptide compared to TAT treatment. No upregulation of TRAIL transcript was observed in any of the peptide treatments (data not shown). GAPDH was used as a loading control. Asterisks denote statistical significance ($p<0.05$). Experiments were run in biological triplicate ($n=3$). Bar graphs represent normalized means ± standard deviation.

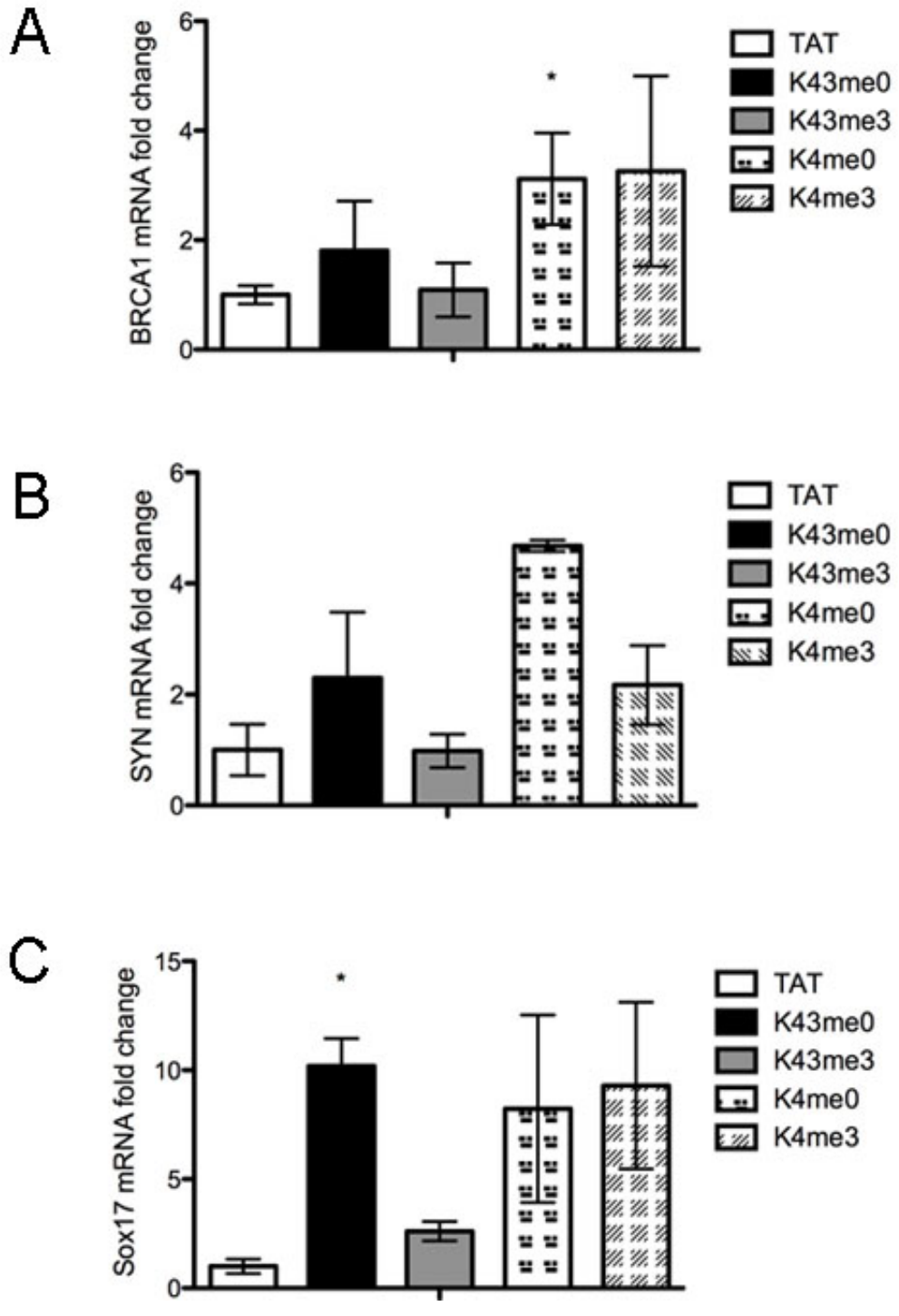
A
BRCA1 mRNA fold change
0
2
4
6
*
TAT
K43me0
K43me3
K4me0
K4me3
B
SYN mRNA fold change
0
2
4
6
TAT
K43me0
K43me3
K4me0
K4me3
C
Sox17 mRNA fold change
0
5
10
15
*
TAT
K43me0
K43me3
K4me0
K4me3

experiments. The absence of apoptosis-inducing factors supports our hypothesis of cell differentiation as a result of KDM5b inhibition and not as a result of cell stress.

2.3.8 Microarray analysis revealed characteristics in peptide-treated ESCs similar to differentiated cells

In order to analyze global changes in gene expression, we employed Gene Ontology (GO) using data from our Affymetrix microarray. A relational graph of phenotypic characteristics was obtained from the array comparing expression patterns of TAT treatment (purple) and H2BK43me0 treatment (green) (Figure 2.8A). The relational graph revealed comparable changes in global gene expression of H2BK43me0 treatment compared to TAT. In addition, we inspected the top five GO categories of global changes between TAT and H2BK43me0. Our results showed that the majority of changes induced by addition of inhibitor peptide compared to control were regulators of transcription (Figure 2.8B). There were comparable global changes in transcription between TAT and H2Bk43me0 cells similar to the changes observed between peptide treatment and day 5 differentiated ESCs. Peptide-induced KDM5b inhibition induced a neural lineage possibly through blocked chromatin recruitment, thus resulting in global changes in transcription similar to when cells differentiate.

2.3.9 H2BK43me0 peptide inhibited KDM5b demethylase activity

Since previous experiments revealed H2BK43me2 as a primary target of KDM5b, we designed an H2BK43 unmethylated peptide as an end-product inhibitor of the demethylase (Stalker et al, 2012). To confirm this interaction, we performed a series of pull-down experiments comparing the binding of recombinant KDM5b (r.KDM5b) to our peptide and to that of H2BK43me2 and the end-product of its alternated substrate, H3K4me0 (Figure 2.9A). Immunoblotting for KDM5b, we revealed maximal pull-down H2BK43me0 and no interaction with its alternate substrates. Our pull-downs confirm H2BK43me0 peptide as an

Figure 2.8 Gene Ontology analysis revealed differences between TAT and H2BK43me0-treated ESCs

Relational graph of phenotypic characteristics shows similarities and differences in global gene expression between TAT control peptide (purple), and H2BK43me2 peptide-treated cells (green). On a global level, samples treated in K43me0 peptide do not share similar gene ontology (GO) terms with TAT treated cells (A). Comparison of the top five GO categories revealed regulation in transcription as the major difference between TAT and K43me0 peptide-treated samples (B). Transcription also represents one of the highest global changes both between TAT and K43me0 as well as between K43me0 and day 5 wildtype ESCs. The key change between peptide treatment and day 5 differentiated ESCs was the shift from regulation of transcriptionally related programs to genes that are involved in cell signaling (phosphorus metabolic process and intracellular signaling cascade). Data represent biological triplicate experiments.

A

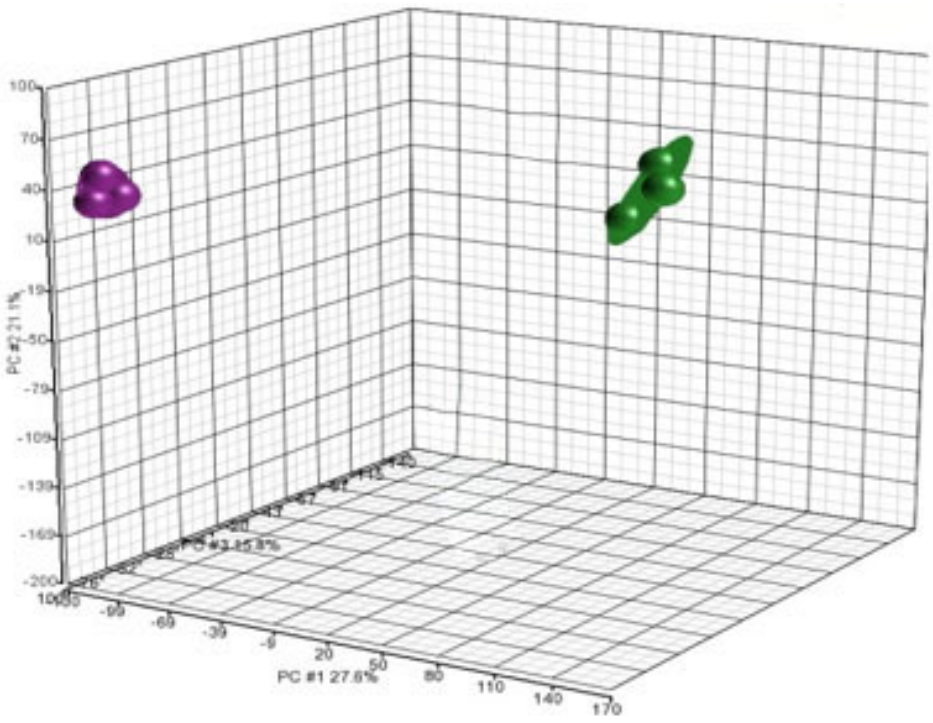

B

Difference between TAT and H2b37-49 Gene ontology categories	% of total genes change	Difference between H2b39-46 and Wt Day 5 Gene ontology categories	% of total genes change
regulation of transcription	18.2	transcription	10.2
transcription	15.7	phosphate metabolic process	5.8
regulation of RNA metabolic process	11.2	phosphorus metabolic process	5.8
regulation of transcription, DNA-dependent	10.9	intracellular signaling cascade	5.8
positive regulation of macromolecule metabolic process	6.2	phosphorylation	5.2

end-product inhibitor of KDM5b demethylase activity that acts to downregulate the enzymatic targeting of other lysine methylation marks. We then examined the expression of transcription factor 3 (TCF3), a known KDM5b target and regulator of self-renewal versus differentiation (Dey et al, 2008). H2BK43me0 peptide treatment significantly upregulated expression of TCF3 transcript compared to control cells ($p<0.05$) (Figure 2.9B). Through chromatin immunoprecipitation (ChIP), we confirmed the downregulation of KDM5b activity at the TCF3 promoter (Figure 2.9C). Furthermore, the inhibition of KDM5b significantly enriched recruitment of H2BK43me2 at TCF3 (Figure 2.9D). Peptide inhibition of KDM5b activity also enriched recruitment of H3K4me3 at the promoter of TCF3 (Figure 2.9E). ChIP experiments confirmed KDM5b enzyme inactivation on its target gene TCF3 and revealed the increased enrichment of KDM5b alternate substrates at this gene.

2.3.10 Peptide treatment upregulated H2BK43me2 recruitment at Egr1 promoter regions

After revealing the activity of KDM5b target gene TCF3, we investigated another target gene involved in differentiation. As a regulator of cell cycle exit and early cell fate, we demonstrated that Egr1 was upregulated during differentiation and when treated with inhibitor peptide (Figure 2.6A,B). We then compared enrichment of H2BK43me2 at Egr1 transcriptional start site (TSS) and TATA region between ESCs and differentiated cells at day 5. ChIP experiments revealed the upregulation of H2BK43me2 at Egr1 TATA when cells were differentiated, but only slightly increased at Egr1 TSS (Figure 2.10A). This trend was similar to the comparison between TAT and H2BK43me0 cells treated for 24 hours (Figure 2.10B). When we examined enrichment at downstream regions of Egr1 such as the 3'UTR and at -1700 to -1920, there was no observable upregulation of H2BK43me2. These findings suggested that peptide-induced cell differentiation upregulated lineage-associated genes through the inhibition of KDM5b and recruitment of H2BK43me2 at target promoter regions.

Figure 2.9 H2BK43me0 peptide inhibits KDM5b and affects transcriptional regulation of TCF3

Pull-down experiments revealed the interaction between inhibitor peptide and r.KDM5b. Top IP His-tag represents loading control. Streptavidin (SA)-tag pull-down of H2BK43me0,2 H2K4me0, and H2A peptides reveals that r.KDM5b-6xHis is maximally pulled down with unmethylated H2BK43 (A). Last lane shows control anti-KDM5b IP. KDM5b target gene TCF3 was examined for changes in RT-PCR versus control. There was significant increase in TCF3 gene expression when cells were incubated with H2BK43me0 peptide when compared to TAT (B). ChIP experiments revealed a downregulation of KDM5b enrichment at the TCF3 promoter (C). Upregulation of enrichment, however, was observed in KDM5b alternate substrates, H2BK43me2 and H3K4me3 (D,E). Data represent percentages of DNA normalized to input DNA compared between control and experimental samples. Asterisks denote statistical significance ($p<0.05$). Experiments were run in biological triplicate (n=3). Bar graphs represent normalized means ± standard deviation.

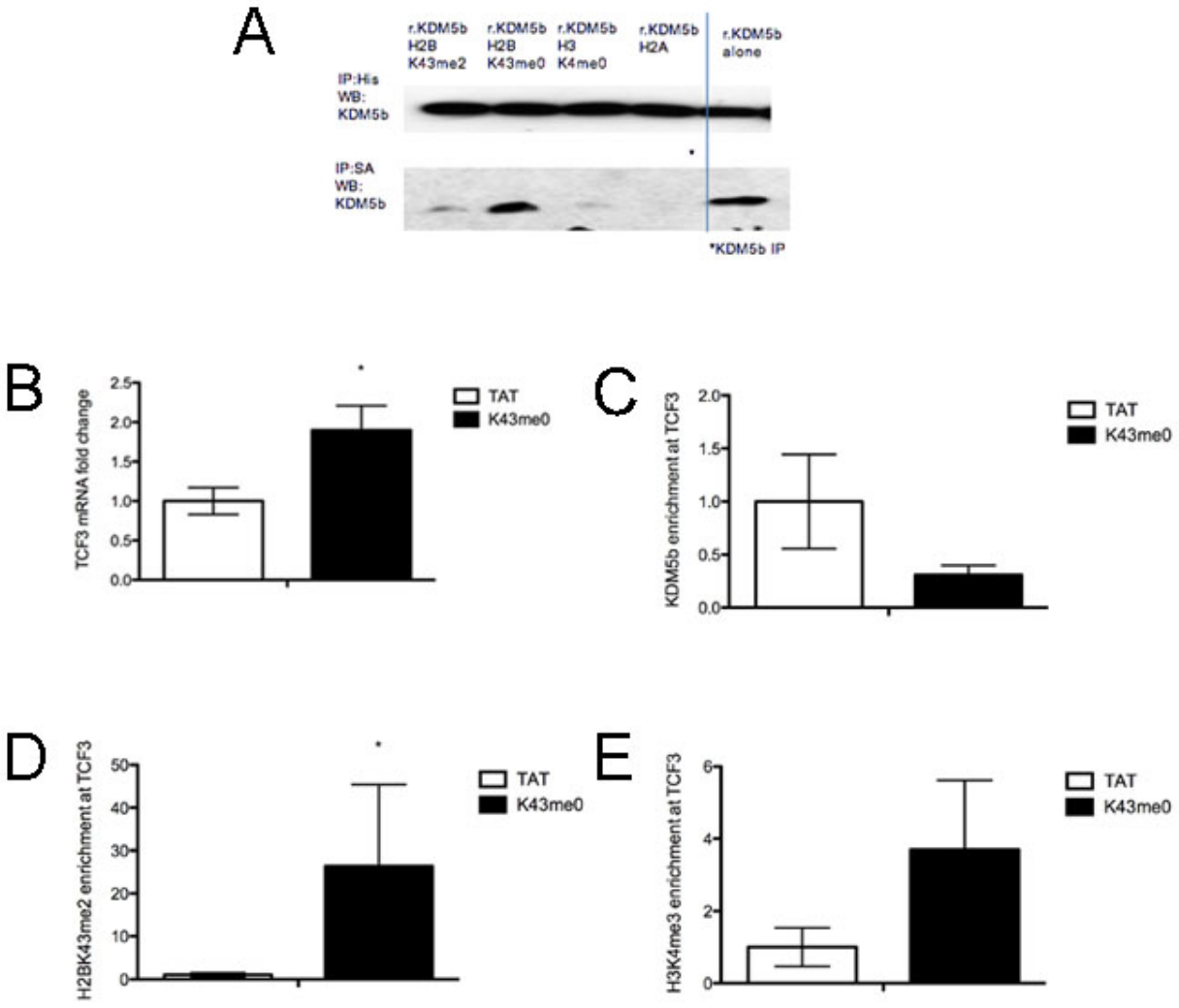
A
r.KDM5b H2B K43me2
r.KDM5b H2B K43me0
r.KDM5b H3 K4me0
r.KDM5b H2A
r.KDM5b alone
IP:His WB: KDM5b
IP:SA WB: KDM5b
*KDM5b IP
B
TCF3 mRNA fold change
TAT
K43me0
C
KDM5b enrichment at TCF3
TAT
K43me0
D
H2BK43me2 enrichment at TCF3
TAT
K43me0
E
H3K4me3 enrichment at TCF3
TAT
K43me0

Figure 2.10 Peptide treatment leads to recruitment of H2BK43me2 at Egr1 promoter regions similar to differentiated cells

Egr1 expression is upregulated early in differentiation and when ESCs were treated with inhibitor peptide. Day 5 differentiated ESCs did not substantially upregulate enrichment of H2BK43me2 at Egr1 transcriptional start site (TSS), but did increase enrichment at Egr1 TATA region when compared to TAT control (A). Similar enrichment patterns were observed between H2BK43me0-treated cells and TAT-treated cells (B). A significant upregulation was seen in peptide-treated cells at the Egr1 TATA region compared to control. There was no increase in H2BK43me2 enrichment at downstream regions of Egr1 promoter. Data represent percentages of DNA normalized to input DNA compared between control and experimental samples. Asterisks denote statistical significance ($p<0.05$). Experiments were run in biological triplicate (n=3). Bar graphs represent normalized means ± standard deviation.

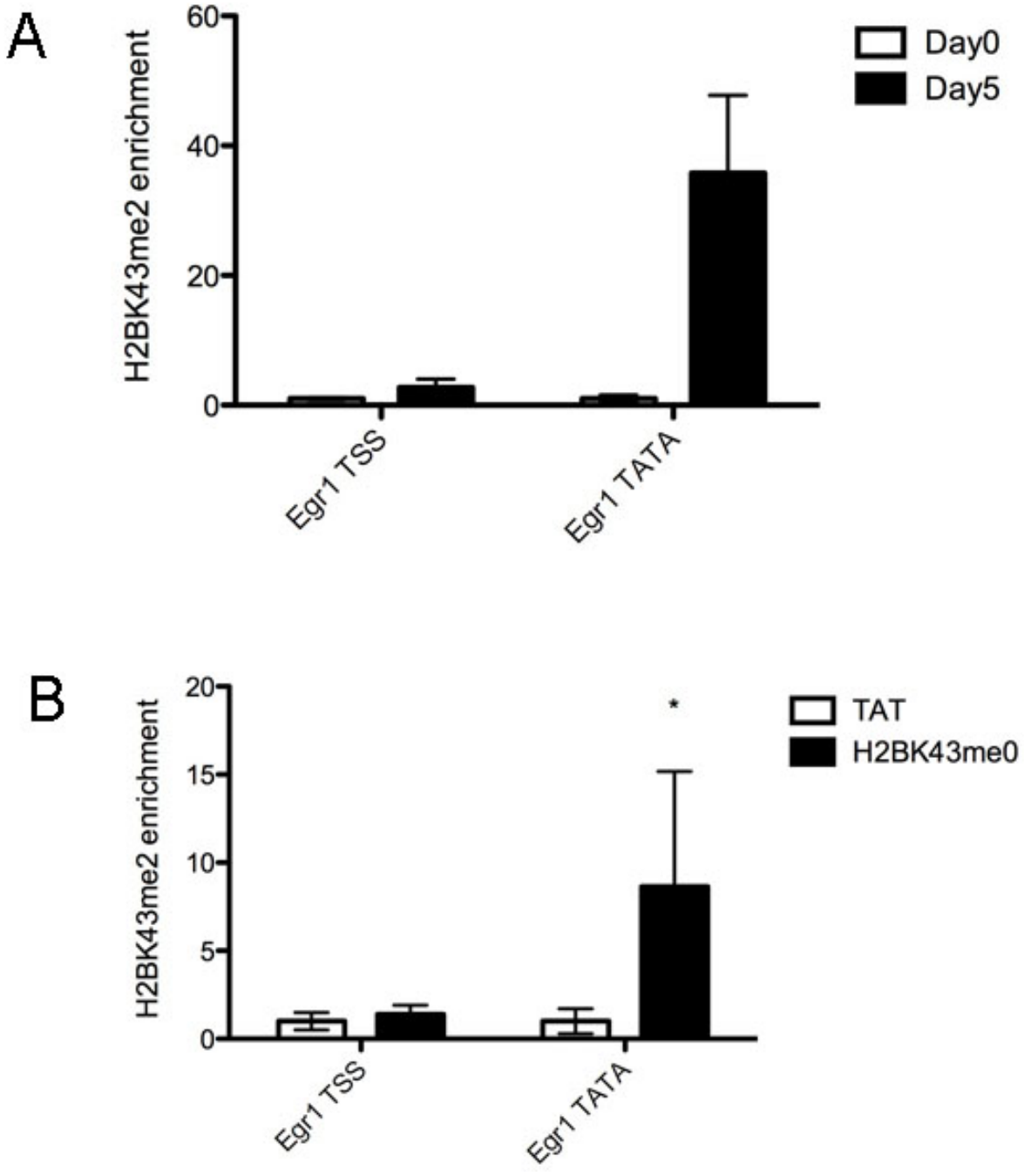
A
H2BK43me2 enrichment
60
40
20
0
Day0
Day5
Egr1 TSS
Egr1 TATA
B
H2BK43me2 enrichment
20
15
10
5
0
*
TAT
H2BK43me0
Egr1 TSS
Egr1 TATA

2.4 Discussion

A variety of histone post-translational modifications impact chromatin remodeling and affect transcriptional regulation of genes (Wu et al 1986). The recruitment of transcription factors and epigenetic control of gene expression is paramount in the proper establishment of the developing embryo (Stein et al 1989). Important pluripotent factors such as Oct4 and Nanog must be maintained at normal levels to ensure proper self-renewal of stem cells (Chambers and Smith 2004, Perry et al 2004). Methylation of histone lysines confers chromatin structural changes and is responsible for epigenetic control of many pluripotent factors, for example the methylation of H3K9 downregulates expression of Oct4 (Freberg et al 2007, Yuan et al 2009). Lysine methylation and demethylation reactions are catalyzed by specific enzymes, KMTs and KDMs (Nochumson et al 1978, Kubicek and Jenuwein 2004). While several KDMs and their substrates remain unidentified, we focus our investigation on the lysine demethylase KDM5b.

As part of the JARID family of Jmjc-domain containing enzymes, KDM5b was originally identified as a factor upregulated in cancer (Lu et al 1999). Further elucidation revealed KDM5b as a lysine-specific demethylase of H3K4 (Schmitz et al 2011). Collaborators of our lab also confirmed KDM5b as a demethylase acting on H2BK43me2 (Stalker et al 2012). Using a novel peptide inhibitor designed to mimic amino acids 37-49 of histone H2B, we hypothesized steric inactivation of KDM5b and the spontaneous differentiation of ESCs. By inhibiting KDM5b enzyme activity, we expected the upregulation of KDM5b target substrates, thus affecting the transcriptional regulation of target genes. In brief, our study revealed the onset of neural differentiation when ESCs were treated with H2BK3me0 peptide. Cells revealed an upregulation of cell cycle and lineage-associated genes, the inhibition of KDM5b at target genes, and the enrichment of KDM5b substrates at target promoters.

2.4.1 Inhibitor peptide localized into ESCs and induced transcriptional changes resulting in differentiation

Our peptides were designed as mimetics of endogenous lysine methylation marks and were

tagged with a nuclear localizing sequence (Frankel and Pablo 1988). Previous localization experiments of TAT peptides were successfully performed in Jurkat T cells and CHO cells (Lundberg and Johannson 2001, Ho et al 2001). Our experiment is the first to demonstrate localization of peptides in mouse embryonic stem cells. Incubating cells with H2BK43me0 peptide initiated ESCs to aggregate and adopt a neurological phenotype. When we investigated transcriptional changes following treatment, we revealed a significant downregulation of pluripotent gene, Nanog. Nanog is a transcription factor well known for its crucial role in embryonic cell fate specification and is immediately downregulated following differentiation (Cavaleri and Scholer 2003). Peptide-induced differentiation is thus partially associated with the decline in Nanog.

An imperative factor for iPS cells, Oct4 remains a central regulator of developmental control. It is well-established that Oct4 must be maintained at adequate levels and the lack of this factor induces trophectoderm differentiation in mouse ESCs (Velkey and O'Shea 2003). In both ESC and EC cells, Oct4 follows a distinct pattern of downregulation following differentiation (Schoorlemmer et al 1995). While there appeared to be downregulation of Oct4 in peptide-treated cells at day 1 of differentiation, we observed minimal changes in Oct4 expression when cells were treated with inhibitor peptide for 24 hours compared to control. Immunofluorescent visualization of Oct4 expression in cells treated with H2BK43me0 for 48 hours revealed positive staining. In previous investigations of Oct4 in ESCs constitutively expressing KDM5b, Dey et al (2008) demonstrated no differences in Oct4 expression compared to control, implying that overexpression of KDM5b did not alter stem cell dynamics. The study also confirmed that when constitutive KDM5b ESCs were differentiated at day 3, cells continued to express Oct4. Taken together, our studies support the conclusion that Oct4 is a late pluripotent marker, observed when ESCs are induced to differentiate. This is in agreement with previous studies identifying Oct4 as an early differentiation marker that is expressed in the embryonic neural crest (Guo et al 2002).

Induced differentiation can often result following cell stress; in fact, apoptosis and differentiation are physiological processes that share several common features (Altman et al 2002, Lanneau et al 2007). Cell differentiation as a result of mechanical stress upregulates many factors involved in apoptosis such as TRAIL (Wu et al 2011, Gobbi et al 2012). To eliminate the possibility of stress-induced differentiation, we ensured that TRAIL was not

upregulated in any of our treatment experiments.

Confirming lineage-specific differentiation, treatment of H2BK43me0 peptide also induced transcriptional upregulation of neural markers. NF is critical for neural structure while neuroD2 plays a role in neurite formation (Lalonde and Strazielle 2003, Messmer et al 2011). TUJ1 is characteristic of embryoid bodies when mouse ESCs are induced to differentiate into the neural lineage in culture (Xu et al 2012). Synapsin is a lineage-associated gene with implications in the regulation of neurotransmitter release at synapses (Esser et al 1998). The appearance of neural markers in our peptide-treated cells confirmed the neuronal differentiation phenotype when ESCs were incubated with H2BK43me0. Another gene that was upregulated during peptide treatment was Sox17, a known transcription factor playing key roles in developmental processes such as endoderm formation, cardiac myogenesis, and the differentiation of neural cells (Combes et al 2012). Increase in Sox17 expression following peptide-induced differentiation of ESCs was consistent with previous studies of upregulation during embryonic development Further investigation is required examining the role of KDM5b regulation and histone post-translational affects on Sox17 gene. Some studies have revealed the role of HDAC inhibition augmenting endoderm differentiation and the possibility of histone acetylation regulating the Sox17 promoter (Fu et al 2011). We are curious to discover if the development gene is subject to lysine methylation and if H3K4 and H3K9 regulate transcriptional expression of Sox17.

2.4.2 H2BK43me0 peptide is an inhibitor of KDM5b and upregulates known target genes

We observed pronounced differentiation characteristics in embryonic stem cells when treated with an inhibitor peptide. Since previous experiments revealed H2BK43me2 as a target of KDM5b demethylase activity, we designed our peptide in the unmethylated state of H2BK43 as an end-product inhibitor of the demethylase enzyme. Many reaction end products are known to sterically inactivate enzymes, for example small molecules have been designed to inhibit HDAC activity in the treatment of cancer (Zhou et al 2011). Furthermore,

monoamine oxidases have been employed as mimics of LSD1 and inhibitors of H3K4 demethylation (Lee et al 2006). In fact, the nonmethylated end product of H3K4 methylation, H3K4me0, acts as a competitive inactivator of LSD1 and inhibits the enzyme from interacting with its substrates (Lan et al 2007). We have demonstrated the pull-down of KDM5b with H2BK43me0 peptide, validating the binding of our peptide with the enzyme and inhibiting interaction with other KDM5b substrates. ESCs treated with the KDM5b inhibitor upregulated target genes including Egr1, BRCA1, and TCF3.

Egr1 is gene known to be involved in cell cycle exit and the early onset of differentiation (Sukhatme et al 1988, Petrovic et al 2010, Lejard et al 2011). Our results are consistent with the literature in that peptide-induced differentiation increased expression of Egr1. This finding is also congruent with previous experiments involving significant decrease of Egr1 in cells overexpressing KDM5b (Dey et al 2008). Egr1 was more sensitive to loss of KDM5b than other cell cycle genes because of its role as an immediate early gene and its variability of expression in mouse ESCs (Waters et al 1990).

KDM5b was originally identified as a factor upregulated in breast cancer (Lu et al 1999). Subsequent studies revealed KDM5b as a lysine demethylase of H3K4 and inhibited the tumor repressor gene BRCA1 (Yamane et al 2007). BRCA1 is involved in DNA damage repair and mutations in the gene confer inherited susceptibility to poor breast cancer prognosis (Easton et al 1993, Bowcock 1993). Consistent with these studies, treatment of KDM5b inhibitor peptide upregulated BRCA1 expression in ESCs. Our findings recapitulate BRCA1 as a target of KDM5b but do not elucidate the role of BRCA1 in stem cell differentiation. Feng and Zhang (2012) propose a role for BRCA1 in the cell cycle eliciting replication blocks, a function that may have relevance in the decision between proliferation and differentiation. In addition, Yoo and Henninghausen (2012) published the contribution of EZH2 methylation at H3K27 in suppressing BRCA1 and affecting cell cycle in breast cancer cells. Other methylation marks may expand our understanding of BRCA1 function in an embryonic stem cell model and imply cross-regulation between cancer, cell cycle, and development.

Transcription factor 3 (TCF3) remains an integral component of the Wnt signaling pathway, controlling lineage differentiation of embryonic stem cells (Watanabe and Dai, 2011). The regulated circuitry of Oct4, Sox2, and Nanog is maintained in tight orchestration to ensure proper timing of cell differentiation (Rodda et al 2005). Cole et al (2008) introduced TCF3 as a co-occupant of promoters throughout the genome in association with Oct4 and Nanog, and demonstrated that TCF3 depletion increases expression of these pluripotency factors. Indeed, TCF3 regulates stem cell dynamics through the inhibition of Nanog, a function that limits self-renewal and promotes cell differentiation (Pereira et al 2006). Through transient transfections of KDM5b in ESCs, Dey et al (2008) identified an increase in the expression of Nanog. The group was unsuccessful in determining TCF3 transcription in KDM5b siRNA experiments. We were able to reveal upregulation of TCF3 expression and downregulation of Nanog when cells were treated with the KDM5b inhibitor peptide. Thus, our experiments confirmed TCF3 as a direct target of KDM5b and the repression of Nanog as a consequence of induced differentiation.

2.4.3 Global gene expression of peptide-treated cells recapitulate changes in KDM5b heterozygous ESCs

GO analysis revealed the primary change in gene expression to be regulation of transcription when comparing cell samples between H2BK43me0 and TAT treatments. Transcriptional changes are also a principle change between ESC and differentiated cells. It is not surprising that the onset of differentiation is associated with changes in transcriptional circuitry. While ESCs constitutively expressing KDM5b were unable to properly form neurons, KDM5b knockdown ESCs differentiation characteristics remained inconclusive (Dey et al 2008). Our lab performed GO analysis on KDM5b heterozygous stem cell line from BayGenomics and found expression pattern changes from EpopooooSCs analogous to the comparison between inhibitor peptide and TAT treatments (data not shown). Relational graph exhibited close correlation of H2BK43me0 peptide-treated cells and KDM5b heterozygous ESCs. When Dey et al attempted to form embryoid bodies with KDM5b heterozygous cells, they observed a high level of apoptosis and could not gather conclusions representative of KDM5b

expression profiles. With GO analysis, we were able to disclose similarities in ESCs treated with KDM5b inhibitor peptide and ESCs heterozygously expressing KDM5b. This similarity in global expression profiles validated our peptide as a KDM5b inhibitor in ESCs. Using a peptide inhibitor-based paradigm, we were able to perform successful experiments in a stem cell model to elucidate the function of histone lysine demethylases.

2.4.4 Recruitment of KDM5b substrates increased in cells treated with inhibitor peptide

Experiments with H2BK43me0 peptide revealed an upregulation of several factors, including BRCA1, Egr1, NF, Sox17, and TCF3. We speculated an interaction of our peptide with KDM5b, inhibiting its demethylase activity and affecting downstream target genes. The inhibition of KDM5b thus explains the increase in expression observed in such targets as BRCA1, Egr1, and TCF3. While the role of BRCA1 in stem cell differentiation remains to be uncovered, TCF3 is a characterized repressor of Nanog and confers regulation of cell specification. Since peptide inhibition of KDM5b resulted in an upreguation of TCF3, we were prompted to investigate enrichment of KDM5b substrates on the promoter of TCF3 gene. KDM5b was previously found to bind to the -50 to -150 region of TCF3 (Dey et al 2003). When ESCs were transfected with KDM5b, Dey et al observed an increase of KDM5b at TCF3. Parallel to this finding, inhibition of the demethylase with H2BK43me0 peptide resulted in a reduced enrichment at TCF3 promoter regions. Our lab also found that on day 0, H3K4me3 and H2BK43me2 are found at downstream regions but are absent from promoter regions. However, when ESCs are differentiated, the two methylation marks enriched at the TSS region of TCF3, while KDM5b is removed (Stalker et al 2012). With chromatin immunoprecipitation, we examined TSS promoter enrichment when cells were treated with KDM5b inhibitor peptide. Our results confirm previous findings in that addition of peptide decreased KDM5b at TCF3 promoter, while H2BK43me2 and H3K4 were enriched at this region compared to control.

While we provided evidence supporting regulation of TCF3, we continued to elucidate the effect of peptide addition on KDM5b targets. Our results are congruent with

preceding experiments in that KDM5b disruption upregulated the expression of Egr1. Overexpression of KDM5b was shown to decrease Egr1 expression, and a 70% decrease of H3K4me3 was observed at the Egr1 promoter (Dey et al 2008). We chose to examine enrichment of the KDM5b alternate substrate, H2BK43me2, at Egr1 promoter regions TSS and TATA. Day 5 differentiated ESCs exhibited an increase of H2BK43me2 enrichment at Egr1 TATA compared to control, while this upregulation was less pronounced at Egr1 TSS. Similar increases at these regions were observed when inhibitor peptide was introduced into culture compared to TAT control. Our findings support Egr1 as a direct target of KDM5b and introduce the upregulation of substrate H2BK43me2 in order to further regulate Egr1 expression as cells differentiate. From our ChIP studies, we speculate that recruitment of H2BK43me2 at target genes mirrors the functional significant of H3K4me3 enrichment at factors involved in species development.

2.4.5 Peptide-induced cell differentiation is specific to H2BK43me0

An immediate neural phenotype was observed when ESCs were treated with H2BK43me0 peptide. On the contrary, treating cells with the trimethylated peptide did not induce any changes when compared to TAT treatment. Furthermore, treatment of H3K4 methylated peptides also failed to induce any morphological changes. H3K4 methylated mark targets many differentiation genes for activation, as previously reviewed (Lee and Shilatifard, 2007, Benevolenskaya 2007). Since H3K4 peptides did not induce differentiation characteristics in ESCs, we propose a compensatory mechanism enabling cells resistant to the treatment of these inhibitor peptides. While H3K4me0 was revealed to be an inhibitor of LSD1 (Lan et al 2007), the enzyme inactivation was insufficient in creating any observable changes in ESCs. When cells were treated with H3K9 methylated peptides, ESCs also remained resistant to morphological changes. H3K9 methylation recognizes promoters for gene silencing and inactivation (Snowden et al 2002). It is uncertain if the end-product peptide can act as a steric inhibitor on enzymes targeting H3K9, but we theorize a tight control of factors associated with this histone mark conferring resistance to the addition of inhibitor peptides. Although we do not observe any perceivable changes in cell morphology when H3K4 and H3K9

peptides were introduced, it is possible that transcriptional changes are occurring. Slight increases in Egr1 expression were observed when cells were treated with H2BK43me3, and lineage-associated factors were upregulated when cells were treated with H3K4 peptides. Further investigation is required in order to understand the possible outcomes and transcriptional changes when other methylated peptides are introduced into ESCs.

References

Adamo A, Sesé B, Boue S, Castaño J, Paramonov I, Barrero MJ, and Izpisua Belmonte JC. (2011). LSD1 regulates the balance between self-renewal and differentiation in human embryonic stem cells. *Nat Cell Biol.* 13:652-659.

Altman GH, Horan RL, Martin I, Farhadi J, Stark PR, Volloch V, Richmond JC, Vunjak-Novakovic G, and Kaplan DL. (2002). Cell differentiation by mechanical stress. *FASEB J.* 16:270-272.

Anderson DC, Green GR, Smith K, and Selker EU. (2010). Extensive and varied modifications in histone H2B of wild-type and histone deacetylase 1 mutant Neurospora crassa. *Biochemistry*. 49:5244-5257.

Bernstein B, Mikkelsen T, Xie X, Kamal M, Hueber D, Cuff J, Fry B, Meissner A, Wernig M, Plath K, Jaenish R, Wagschal A, Feil R, Schreiber S, and Lander ES. (2006). A bivalent chromatin structure marks key developmental genes in embryonic stem cells. *Cell*. 125:315-326.

Benevolenskaya EV. (2007). Histone H3K4 demethylases are essential in development and differentiation. *Biochem Cell Biol.* 85:435-443.

Bowcock AM. (1993). Molecular cloning of BRCA1: a gene for early onset familial breast and ovarian cancer. *Breast Cancer Res Treat*. 28:121-135.

Cavaleri F, Scholer HR. (2003). Nanog: a new recruit to the embryonic stem cell orchestra. *Cell*. 113:551-552.

Chambers I, Smith A. (2004). Self-renewal of teratocarcinoma and embryonic stem cells. *Oncogene*. 23:7150-7160.

Collins K, Jacks T, and Pavletich NP. (1997). The cell cycle and cancer. *PNAS.* 94:2776-2778.

Combes P, Planche V, Eymard-Pierre E, Sarret C, Rodriguez D, Boespflug-Tanguy O, and Vaurs-Barriere C. (2012). Relevance of SOX17 Variants for Hypomyelinating Leukodystrophies and Congenital Anomalies of the Kidney and Urinary Tract (CAKUT). *Ann Hum Genet*. 10:1469-1809.

Dey BK, Stalker L, Schnerch A, Bhatia M, Taylor-Papidimitriou J, and Wynder C. (2008.) The Histone Demethylase KDM5b/JARID1b plays a role in cell fate decisions by blocking terminal differentiation. *Mol Cell Biol,* 28:5312–5327.

Easton D, Ford D, and Peto J. (1993). Inherited susceptibility to breast cancer. *Cancer Surv.* 18:95-113.

Esser L, Wang CR, Hosaka M, Smagula CS, Südhof TC, and Deisenhofer J. (1998). Synapsin I is structurally similar to ATP-utilizing enzymes. *EMBO J.* 17:977–84.

Feng Z, Zhang J. (2012). A dual role of BRCA1 in two distinct homologous recombination mediated repair in response to replication arrest. *Nucleic Acids Res.* N40:726-738.

Frankel AD, and Pabo CO. (1988). Cellular uptake of the tat protein from human immunodeficiency virus. *Cell.* 55:1189-1193.

Freberg CT, Dahl JA, Timoskainen S, and Collas P. (2007). Epigenetic reprogramming of OCT4 and NANOG regulatory regions by embryonal carcinoma cell extract. *Mol Biol Cell.* 18:1543-1553.

Fu S, Fei Q, Jiang H, Chuai S, Shi S, Xiong W, Jiang L, Lu C, Atadja P, Li E, and Shou J. (2011). Involvement of histone acetylation of Sox17 and Foxa2 promoters during mouse definitive endoderm differentiation revealed by microRNA profiling. *PLoS One.* 6:e27965.

Gobbi G, Di Marcantonio D, Micheloni C, Carubbi C, Galli D, Vaccarezza M, Bucci G, Vitale M, and Mirandola P. (2012). TRAIL up-regulation must be accompanied by a reciprocal PKCε down-regulation duringdifferentiation of colonic epithelial cell: implications for colorectal cancer cell differentiation*. J Cell Physiol.* 227:630-8.

Guo Y, Costa R, Ramsey H, Starnes T, Vance G, Robertson K, Kelley M, Reinbold R, Scholer H, and Hromas R. (2003). The embryonic stem cell transcription factors Oct-4 and

FoxD3 interact to regulate endodermal-specific promoter expression. *Proc Natl Acad Sci.* 99:3663-3667.

Herz H, Nakanishi S, and Shilatifard A. (2009). The curious case of bivalent marks. Dev *Cell*. 17:301-303.

Ho A, Schwarze SR, Mermelstein SJ, Waksman G, and Dowdy SF. (2001). Synthetic protein transduction domains: enhanced transduction potential in vitro and in vivo. *Cancer Res*. 61:474-7.

Kubicek S and Jenuwein T. (2004). A crack in histone lysine methylation. *Cell*. 119:903-906.

Lalonde R and Strazielle C. (2003). "Neurobehavioral characteristics of mice with modified intermediate filament genes". *Rev Neurosci* 14:369–385.

Lan F, Collins RE, De Cegli R, Alpatov R, Horton JR, Shi X, Gozani O, Cheng X, and Shi Y. (2007). Recognition of unmethylated histone H3 lysine 4 links BHC80 to LSD1-mediated gene repression. *Nature*. 448:718-722.

Lanneau D, de Thonel A, Maurel S, Didelot C, and Garrido C. (2007). Apoptosis versus cell differentiation: role of heat shock proteins HSP90, HSP70 and HSP27. *Prion* 1:53-60.

Lee JS, and Shilatifard A. (2007). A site to remember: H3K36 methylation a mark for histone deacetylation. *Mutat Res.* 618:130-134.

Lee MG, Wynder C, Schmidt DM, McCafferty DG, and Shiekhattar R. (2006). Histone H3 lysine 4 demethylation is a target of nonselective antidepressive medications. *Chem Biol*. 6:563-567.

Lejard V, Blais F, Guerquin MJ, Bonnet A, Bonnin MA, Havis E, Malbouyres M, Bidaud CB, Maro G, Gilardi-Hebenstreit P, Rossert J, Ruggiero F, and Duprez D. (2011). EGR1 and EGR2 involvement in vertebrate tendon differentiation. *J Biol Chem.* 286:5855-5867.

Li HJ. (1975).A model for chromatin structure. *Nucleic Acids Res.* 2:1275-89.

Lluis F, Ombrato L, Pedone E, Pepe S, Merrill BJ, and Cosma MP. (2006). T-cell factor 3 (Tcf3) deletion increases somatic cell reprogramming by inducing epigenome modifications. *Proc Natl Acad Sci.* 108:11912-11917.

Lu PJ, Sundquist K, Baeckstrom D, Poulsom R, Hanby A, Meier-Ewert S, Jones T, Mitchell M, Pitha-Rowe P, Freemont P, and Taylor-Papadimitriou J. (1999). A novel gene (PLU-1) containing highly conserved putative DNA/chromatin binding motifs is specifically up-regulated in breast cancer. *J. Biol. Chem.* 274:15633–15645.

Lundberg L and Johansson M. (2001). Is VP22 nuclear homing an artifact? *Nat Biotechnol.* 19:713–714.

Messmer K, Shen WB, Remington M, andFishman PS. (2011). Induction of neural differentiation by the transcription factor NeuroD2. *Int J Dev Neurosci.* 30:105–112.

Nochumson S, Kim S, Paik WK. (1978). The methylation and demethylation of protein lysine residues. *Methods Cell Biol.* 19:69-77.

Pereira L, Yi F, and Merrill BJ. (2006). Repression of Nanog Gene Transcription by Tcf3 Limits Embryonic Stem Cell Self-Renewal. *Mol Cell Biol.* 26:7479-7491.

Petrovic I, Kovacevic-Grujicic N, and Stevanovic M. (2010). Early growth response protein 1 acts as an activator of SOX18 promoter. *Exp Mol Med.* 42:132-42.

Phang-Lang C, Scully P, Shew JY, Wang JYJ, and Lee WH. (1989). Phosphorylation of the retinoblastoma gene product is modulated during the cell cycle and cellular differentiation. *Cell.* 58:1193-1198.

Perry P, Sauer S, Billon N, Richardson WD, Spivakov M, Warnes G, Livesey FJ, Merkenschlager M, Fisher AG, and Azuara V. (2004). A dynamic switch in the replication timing of key regulator genes in embryonic stem cells upon neural induction. *Cell Cycle*. 12:1645-1150.

Rodda DJ, Chew JK, Lim LH, Loh YH, Wang B, Ng HH, and Robson P. (2005). Transcriptional regulation of Nanog by Oct4 and Sox2. *J Biol Chem.* 280:2431-2437.

Schmitz S, Albert M, Malatesta M, Morey L, Johansen J, Bak M, Tommerup N, Abarrategui I, and Helin K. (2011). Jarid1b targets genes regulating development and is involved in neural differentiation. *EMBO J.* 30:4586-4600.

Schoorlemmerv J, Jonk L, Shen S, van Puijenbroek A, Feijen A, and Kruijer W. (1995). Regulation of Oct-4 gene expression during differentiation of EC cells *Mol Biol Rep*. 21:129-40.

Shilatifard A. (2008) Molecular implementation and physiological roles for histone H3 Lysine 4 (H3K4) methylation. *Cell*. 20:341-348.

Snowden AW, Gregory PD, Case CC, and Pabo CO. (2002). Gene-specific targeting of H3K9 methylation is sufficient for initiation repression in vivo. *Curr Biol.* 12:2159-2166.

Stalker L, Galka M, Liu H, Keating S, Doughty ML, Truant R, Li SS, and Wynder C. (2012). KDM5b localization to target genes is regulated by a novel histone modification; H2BK43me2. Manuscript submitted for publication (copy on file with author).

Stein GS, Stein JL, Lian JB, Van Wijnen AJ, Wright KL, and Pauli U. (1989). Modifications in molecular mechanisms associated with control of cell cycle regulated humanhistone gene expression during differentiation. *Cell Biophys*. 15:201-223.

Sukhatme VP, Cao X, Chang LC, Tsai-Morris CH, Stamenkovich D, Ferreira PCP, Cohen DR, Edwards SA, Shows TB, Curran T, Le Beau MM, Adamson ED. (1988). A zinc finger-encoding gene coregulated with c-fos during growth and differentiation, and after cellular depolarization. *Cell*. 53:37-43.

Tremml G, Singer M, and Malavarca R. (2008). Culture of Mouse Embryonic Stem Cells. *Curr Protoc Stem Cell Biol.* 5:1C.4.1–1C.4.19.

Varier RA, and Timmers HT. (2011). Histone lysine methylation and demethylation pathways in cancer. *Biochim Biophys Acta.* 1815:75-89.

Velkey MV and O'Shea KS. (2003). Oct4 RNA interference induces trophectoderm differentiation in mouse embryonic stem cells. *Genesis.* 37:18-24.

Vives E, Brodin P, and Lebleu B. (1997). A truncated HIV-1 Tat protein basic domain rapidly translocates through the plasma membrane and accumulates in the cell nucleus. *J Biol Chem.* 272:16010-16017.

Xiang Y, Zhu Z, Han G, Ye X, Xu B, Peng Z, Ma Y, Yu Y, Lin H, Chen AP, and Chen CD. (2007). JARID1B is a histone H3 lysine 4 demethylase up-regulated in prostate cancer. *Proc. Natl. Acad. Sci*. 104:19226–19231.

Watanabe K and Dai X. (2011). A WNTer Revisit: New Faces of β-Catenin and TCFs in pluripotency. *Sci. Signal.* 4:pe41.

Waters CM, Hancock DC, and Evan GI. (1990). Identification and characterisation of the egr-1 gene product as an inducible, short-lived, nuclear phosphoprotein. *Oncogene*. 5:669-674.

Wu NL, Lee TA, Tsai TL, and Lin WW. (2011). TRAIL-induced keratinocyte differentiation requires caspase activation and p63 expression. *J Invest Dermatol.* 131:874-83.

Wu RS, Panusz HT, Hatch CL, and Bonner WM. (1986). Histones and their modifications. *CRC Crit Rev Biochem*. 20:201-263.

Xiong L, Adhvaryu KK, Selker EU, and Wang Y. (2010). Mapping of lysine methylation and acetylation in core histones of Neurospora crassa. *Biochemistry.* 49:5236-5243.

Xu J, Wang H, Liang T, Cai X, Rao X, Huang Z, and Sheng G. (2012). Retinoic acid promotes neural conversion of mouse embryonic stem cells in adherent monoculture. *Mol Biol Rep*. 39:789-795.

Yamane K, Tateishi K, Klose RJ, Fang J, Fabrizio LA, Erdjument-Bromage H, Taylor-Papadimitriou J, Tempst P, and Zhang Y. (2007). PLU-1 is an H3K4 demethylase involved in transcriptional repression and breast cancer cell proliferation. *Mol. Cell.* 25:801–812.

Yoo KH and Hennighausen L. (2012). EZH2 methyltransferase and H3K27 methylation in breast cancer. *Int J Biol Sci.* 8:59-65

Yuan P, Han J, Guo G, Orlov YL, Huss M, Loh YH, Yaw LP, Robson P, Lim B, and Ng HH. (2009). Eset partners with Oct4 to restrict extraembryonic trophoblast lineage potential in embryonic stem cells. *Genes Dev*. 23:2507-2520.

Zhou Q, Dalgard CL, Wynder C, and Doughty ML. (2011). Histone deacetylase inhibitors SAHA and sodium butyrate block G1-to-S cell cycle progression in neurosphere formation by adult subventricular cells. *BMC Neurosci.* 12:50.

Chapter 3

3 General Overview

3.1 Conclusion and Summary

Objective 1. Examine phenotypic changes in ESCs and during differentiation following introduction of inhibitor peptide

Frankel and Pabo (1998) revolutionized the prospects of drug delivery using the TAT sequence derived from HIV. Investigators have successfully localized small molecules into the nucleus of cells using the TAT sequence (Vives et al 1997, Ho et al 2001). While previous localization experiments were performed in cancer cell lines, we have successfully demonstrated the localization of TAT-tagged peptides in mouse ESCs. In order to investigate histone lysine methylation properties in stem cells, we designed a peptide corresponding to amino acids 37-49 of histone H2B. We speculate that the nonmethylated peptide is an end-product inhibitor of the lysine-specific methylase acting on lysine 43 of histone H2B. This common inhibitor-based paradigm has proven successful in inhibition of HDACs as well as the inhibition of H3K4 methylation (Lan et al 2007, Zhou et al 2011). Epigenetic regulation of genes has transpired as a new topic in biological research and many groups strive to fully elucidate the histone code. As more lysine modifications are revealed, associated methyltransferase and demethylase enzymes are also emerging. KDM5b was re-identified when it was revealed to be a lysine demethylase in addition to being a factor upregulated in cancer (Yamane et al 2007, Xiang et al 2007). While KDM5b was initially branded as an H3K4-specific demethylase, our lab revealed the interaction between KDM5b and a novel histone mark, H2BK43me2. Very little work has been performed on histone H2B and virtually no information is known about its role in eukaryotic development. Our synthetic peptide strives to elucidate the role of H2BK43 methylation in stem cells through the inhibition of its lysine demethylase.

When ESCs were incubated with inhibitor peptide, changes in cell morphology were immediately seen. Cells aggregated within hours of treatment and formed neurospheres within 24 hours. The accelerated differentiation following peptide treatment represents a novel method of enzyme inhibition. KDM5b heterozygous ESCs were unable to complete the differentiation time-course and thus offered no conclusive results involving downstream transcriptional dynamics (Dey et al 2008). Inhibition of KDM5b with a synthetic peptide is the first successful experiment inactivating the enzyme's demethylase activity. Interestingly, no phenotypic changes were observed when cells were incubated with H2BK43me3 peptide, confirming end-product inhibition specificity. Similarly, methylated peptides of H3K4 and H3K9 did not confer any morphological changes in stem cells. As two pivotal histone marks of gene activation and repression, we presume that there exists a compensatory mechanisms that enables ESCs to resist morphological changes when treated with H3K4 or H3K9 peptides. Through this novel experiment, we were able to reveal pronounced differentiation phenotypes in stem cells treated specifically with H2BK43me0 peptide.

Objective 2. Investigate transcriptional changes in pluripotent, cell cycle, and lineage-associated genes when cells are treated with H2BK43me0 peptide

Differentiation of embryonic stem cells conforms to a stringently orchestrated downregulation of pluripotent factors such as Oct4 and Nanog (Kashyap et al 2009, Chan et al 2011, Lee and Qu 2011). Following observations of phenotypic differentiation in ESCs treated with H2BK43me0 peptide, we assayed for transcriptional changes of several genes involved in self-renewal and lineage association. Few cells in developed organisms remain in an actively proliferating state; the majority of cells have undergone cell cycle exit. At each mitotic division, ESCs must choose between proliferation and differentiation (Browna et al 2003, Xia et al 2006). Egr1 is an early marker of differentiation and controls many target genes involved in cell cycle progression (Virolle et al 2003). We observed an upregulation in Egr1 expression from days 0 to 3 of differentiation in control and peptide-treated cells. Additionally, a significant increase was observed in H2BK43me0-treated cells compared to TAT-treated ESCs. Upregulation of Egr1 confirmed its role in cell cycle exit, cell

differentiation, and as a target of KDM5b. On the contrary, we did not observe significant downregulation of pluripotent factor Oct4, although a significant decrease in Nanog expression was apparent. Our results confirm Nanog as a gene immediately downregulated following differentiation, while Oct4 remains a late pluripotent marker expressed in neural crest cells (Guo et al 2003).

In tandem with upregulation of Egr1, cells treated with inhibitor peptide increased expression of several lineage-associated genes indicative of a neural phenotype. Peptide treatment promoted upregulation of NF, neuroD2, TUJ1 and Synapsin expression levels. Since these markers are imperative in the structural and functional integrity of neural cells, we conclude that ESCs treated with inhibitor peptide have adopted a neural lineage. KDM5b heterozygous ESCs failed to express neural markers when differentiated toward the neural lineage (Dey et al 2008). While increasing KDM5b obstructed differentiation of stem cells, treatment of the KDM5b inhibitor peptide encouraged the differentiation of cells and upregulated several neural-associated factors. In addition to neural genes, peptide treatment also increased the expression of other lineage genes such as Sox17. As a factor involved in endoderm formation, Sox17 upregulation is consistent with differentiation phenotype observed in ESCs following peptide treatment. The possibility of Sox17 epigenetic regulation was introduced by Fu et al (2011); the study revealed Sox17 regulation via histone acetylation and the role of HDAC inhibitors in enhancing endodermal differentiation. Possible lysine methylation mechanisms may also offer regulatory control of such differentiation genes such as the Sox family of transcription factors.

Objective 3. Characterize the interaction of our peptide with KDM5b and its effect on alternate substrates and downstream target genes

While initial studies involving KDM5b lysine demethylase involved H3K4, investigations in our lab confirmed an additional histone target, H2BK43me2 (Yamane et al 1997, Stalker et al 2012). KDM5b maximally pulled down our unmethylated H2BK43me0 peptide and inhibited interaction with other substrates of the demethylase. KDM5b enzyme disruption thus increased enrichment of H2BK43me2 as well as H3K4me3 at target genes. When we examined KDM5b targets following H2BK43me0 peptide incubation, we observed an

increase in BRCA1 and TCF3 expression. Upregulation in breast cancer tumor suppressor gene BRCA1 confirmed speculation of its interaction with KDM5b (Lu et al 1999, Yamane et al 2007). Close inspection of the TCF3 gene revealed significant increase in ESCs treated with peptide compared to control. Furthermore, peptide treatment reduced KDM5b activity at TCF3 promoter. Constitutive KDM5b in ESCs was previously shown to increase the enzyme interaction with TCF3 (Dey et al 2008). Our ChIP assays also demonstrate the upregulation of KDM5b substrates, H2BK43me2 and H3K4me3 at the TCF3 promoter regions. Taken together, we deduce a synergistic mechanism of regulating transcriptional factors. H2BK43me2 recruitment may mirror the effects of H3K4me3 activation on target genes such as TCF3. Co-occupancy of TCF3 at pluripotent genes such as Nanog indicates that TCF3 plays an integral role in Wnt-dependent stimulation of self-renewal in stem cells (Yi et al 2011).

Additional ChIP experiments compared the enrichment of H2BK43me2 at Egr1 promoter regions between ESCs and day 5 differentiated cells. While a slight increase occurred at Egr1 TSS, a substantial upregulation was observed at the Egr1 TATA region. Comparison of TAT and H2BK43me0 peptide-treated ESCs also reflected this trend in upregulation, with a significant increase of the dimethylated lysine mark at Egr1 TATA. These findings agree with overexpression experiments of KDM5b in ESCs, in which a reduction of H3K4me3 was seen at the Egr1 gene promoter while an upregulation of KDM5b at Egr1 occurred (Dey et al 2008). Transient siRNA-mediated knockdown experiments of KDM5b also increased levels of H3K4me3 at Egr1, similar to our peptide-inhibited assays. Downregulation of KDM5b at target genes and upregulation of substrates at the same target regions reveal the cooperation of lysine demethylases and their respective histone marks in regulating transcription. Investigations using H2B inhibitor peptide have confirmed H2BK43me2 as a crucial mark in the histone code and an integral contender in the circuitry involved in organism development.

3.2 Future studies

In our screen of 88 peptides with varying methylation states, we found that most peptides did not elicit phenotypic abnormalities when cultured with ESCs. While H2BK43me0 was

capable of inducing differentiation, the trimethylated peptide of the same lysine did not generate any cell changes compared to TAT control. ESCs incubated with peptides of other important histone marks such as H3K4 and H3K9 also retained stem cell qualities and were resistant to change. Although no observable differences were exhibited when cells were viewed under a microscope, transcriptional dynamics may have been altered with treatment of alternate peptides. In fact, H2BK43me3 appears to upregulate Egr1 when introduced in cell culture. H3K4 peptides also seem to increase expression of a few lineage genes such as Sox17. Recent studies in biochemical research have revealed methods of inhibiting important histone post-translational modifications in order to determine functional relevance of these marks. For example, the use of oligoamine analogues to inhibit LSD1 and induce expression of epigenetically silenced genes, or the analogue BIX-01294 in suppressing G9a activity on H3K9 (Huang et al 2009, Upadhyay et al 2012). Since H3K4 and H3K9 are imperative for epigenetic gene regulation, alterations in transcriptional dynamics may be rectified by alternate mechanisms in order to maintain integrity of the developing embryo (Eissenberg and Shilatifard 2010, Shinkai 2007). This could explain why changes in lineage genes are seen but ESCs are resistant to phenotypic changes when treated with H3K4 or H3K9 inhibitor peptides. In addition to these two histone lysines, several other marks remain undiscovered. Our large-screen assay revealed the promising possibilities that H3K23 and H4K20 may participate in developmental regulation. Further investigations of self-renewal genes following treatment of these peptides may provide us with a clearer picture of the complete histone code.

In terms of the interaction between the inhibitor peptide and KDM5b, future studies may provide details of steric inactivation of the enzyme. In the case of H3K4me0 binding BHC80, substrate specificity is conferred through a hydrogen bond “cage” recognition of the H3 amino terminus (Lan et al 2007). Monomethylated lysine allowed limited motion before clashing with other atoms, thus additional methyl groups on H3K4 would interfere with side chains of the enzyme. While we were able to show binding of our peptide to KDM5b and the out-competing of alternate lysine substrates, further investigations in protein crystallography would elucidate sites of steric inhibition and enzyme suppression. While we have focused our study in a stem cell model of development, many factors we investigated have dual roles in differentiation and cell cycle regulation. This suggests that KDM5b inhibition at target genes

may have implications in cancer cell lines as well. KDM5b was originally identified upregulated in cancers and targets transcription of tumor suppressor genes such as BRCA1 (Lu et al 1999, Yamane et al 2007, Xiang et al 2007). Egr1 is responsible for cell cycle exit, early differentiation, and is involved in cancer cell signaling (Liu et al 1998, Song et al 2012). The knockdown of KDM5b and upregulation of tumor-associated genes BRCA1 and Egr1 would potentially alter signaling landscapes in cancer cells and confer therapeutic outcomes. Mutation in BRCA1 is often associated with poor prognosis and studies strive to target the gene for upregulation in patients (Clark-Knowles et al 2010). This offers the possibility of KDM5b inhibition as a potential target in future cancer therapy. Results from stem cells can hopefully be extrapolated to cancerous cell lines; however, further experimentation of KDM5b regulation in a tumorigenetic model must be performed to better understand the onset of cancer from an epigenetic viewpoint.

References

Browna G, Hughesa PJ, and Michell RH. (2003). Cell differentiation and proliferation—simultaneous but independent? *Exp Cell Res.* 291:282–288.

Chan YS, Yang L, and Ng HH. (2011). Transcriptional regulatory networks in embryonic stem cells. *Prog Drug Res*. 67:239-52.

Dey BK, Stalker L, Schnerch A, Bhatia M, Taylor-Papidimitriou J, and Wynder C. (2008.) The Histone Demethylase KDM5b/JARID1b plays a role in cell fate decisions by blocking terminal differentiation. *Mol Cell Biol,* 28:5312–5327.

Eissenberg JC, and Shilatifard A. (2010). Histone H3 lysine 4 (H3K4) methylation in development and differentiation. *Dev Biol.* 339:240-249.

Frankel AD, and Pabo CO. (1988). Cellular uptake of the tat protein from human immunodeficiency virus. *Cell.* 55:1189-1193.

Fu S, Fei Q, Jiang H, Chuai S, Shi S, Xiong W, Jiang L, Lu C, Atadja P, Li E, and Shou J. (2011). Involvement of histone acetylation of Sox17 and Foxa2 promoters during mouse definitive endoderm differentiation revealed by microRNA profiling. *PLoS One.* 6:e27965.

Guo Y, Costa R, Ramsey H, Starnes T, Vance G, Robertson K, Kelley M, Reinbold R, Scholer H, and Hromas R. (2003). The embryonic stem cell transcription factors Oct-4 and FoxD3 interact to regulate endodermal-specific promoter expression. *Proc Natl Acad Sci.* 99:3663-3667.

Ho A, Schwarze SR, Mermelstein SJ, Waksman G, and Dowdy SF. (2001). Synthetic protein transduction domains: enhanced transduction potential in vitro and in vivo. *Cancer Res*. 61:474-7.

2009 Dec 1;15(23):7217-28. Epub 2009 Nov 24.

Huang Y, Stewart TM, Wu Y, Baylin SB, Marton LJ, Perkins B, Jones RJ, Woster PM, and Casero RA Jr. (2009). Novel oligoamine analogues inhibit lysine-specific demethylase 1 and induce reexpression of epigenetically silenced genes. *Clin Cancer Res.* 15:7217-7228.

Kashyap V, Rezende NC, Scotland KB, Shaffer SM, Persson JL, Gudas LJ, and Mongan NP. (2009). Regulation of stem cell pluripotency and differentiation involves a mutual regulatory circuit of the NANOG, OCT4, and SOX2 pluripotency transcription factors with polycomb repressive complexes and stem cell microRNAs. *Stem Cells Dev*. 18:1093-1098.

Lee YH, and Wu Q. (2011). Chromatin regulation landscape of embryonic stem cell identity. *Biosci Rep.* 31:77-86.

Liu C, Rangnekar VM, Adamson E, and Mercola D. (1998). Suppression of growth and transformation and induction of apoptosis by EGR-1. *Cancer Gene Ther.* 5:3-28.

Lu PJ, Sundquist K, Baeckstrom D, Poulsom R, Hanby A, Meier-Ewert S, Jones T, Mitchell M, Pitha-Rowe P, Freemont P, and Taylor-Papadimitriou J. (1999). A novel gene (PLU-1) containing highly conserved putative DNA/chromatin binding motifs is specifically up-regulated in breast cancer. *J. Biol. Chem.* 274:15633–15645.

Shinkai Y. (2007). Regulation and function of H3K9 methylation. *Subcell Biochem.* 41:337-350.

Stalker L, Galka M, Liu H, Keating S, Doughty ML, Truant R, Li SS, and Wynder C. (2012). KDM5b localization to target genes is regulated by a novel histone modification; H2BK43me2. Manuscript submitted for publication (copy on file with author).

Upadhyay AK, Rotili D, Han JW, Hu R, Chang Y, Labella D, Zhang X, Yoon YS, Mai A, and Cheng X. (2012). An analog of BIX-01294 selectively inhibits a family of histone H3 lysine 9 Jumonji demethylases. *J Mol Biol.* 416:319-327.

Virolle T, Krones-Herzig A, Baron V, De Gregorio G, Adamson ED, and Mercola D. (2003). Egr1 promotes growth and survival of prostate cancer cells. Identification of novel Egr1 target genes. *J Biol Chem. 278*:11802-11810.

Vives E, Brodin P, and Lebleu B. (1997). A truncated HIV-1 Tat protein basic domain rapidly translocates through the plasma membrane and accumulates in the cell nucleus. *J Biol Chem.* 272:16010-16017.

Xia K, Xue H, Dong D, Zhu S, Wang J, Zhang Q, Hou L, Chen H, Tao R, Huang Z, Fu Z, Chen YG, and Han JDJ. (2006). Identification of the proliferation/differentiation switch in the cellular network of multicellular organisms. *PLoS Comput Biol.* 2:e145.

Xiang Y, Zhu Z, Han G, Ye X, Xu B, Peng Z, Ma Y, Yu Y, Lin H, Chen AP, and Chen CD. (2007). JARID1B is a histone H3 lysine 4 demethylase up-regulated in prostate cancer. *Proc. Natl. Acad. Sci.* 104:19226–19231.

Yamane K, Tateishi K, Klose RJ, Fang J, Fabrizio LA, Erdjument-Bromage H, Taylor-Papadimitriou J, Tempst P, and Zhang Y. (2007). PLU-1 is an H3K4 demethylase involved in transcriptional repression and breast cancer cell proliferation. *Mol. Cell.* 25:801–812.

Yi F, Pereira L, Hoffman JA, Shy BR, Yuen CM, Liu DR, and Merrill BJ. (2011). Opposing effects of Tcf3 and Tcf1 control Wnt stimulation of embryonic stem cell self-renewal. *Nat Cell Biol*. 13:762-1770.

Zhou Q, Dalgard CL, Wynder C, and Doughty ML. (2011). Histone deacetylase inhibitors SAHA and sodium butyrate block G1-to-S cell cycle progression in neurosphere formation by adult subventricular cells. *BMC Neurosci.* 12:50.

Curriculum Vitae

Name: Wendy Zhu

Post-secondary Education and Degrees:

DMD Candidate, Boston University
Henry M. Goldman School of Dental Medicine
Boston, Massachusetts, USA
2012-2016

MSc Candidate, University of Western Ontario
Schulich School of Medicine and Dentistry
London, Ontario, Canada
Department of Biochemistry, Supervisor Dr. Shawn Li
2009-2012

BSc Awarded, University of Western Ontario
London, Ontario, Canada
Honours Specialization in Cell and Developmental Biology
2005-2009

Honours and Awards:

Schulich Scholarship for Medical Research
2010-2011

Western Graduate Research Scholarship
2009-2010

Related Work Experience

Research Assistant
Lawson Health Research Institute
Department of Medical Biophysics
2009-2010

Research Assistant
The University of Western Ontario
Department of Physiology and Pharmacology
2009

Publications:

Mitchell AJ, Sabondjian E, Sykes J, Deans L, Zhu W, Lu X, Feng Q, Prato FS, Wisenberg G. (2010). Comparison of initial cell retention and clearance kinetics after subendocardial or subepicardial injections of endothelial progenitor cells in a canine myocardial infarction model. *J Nucl Med.* 51:413-417.